Tu-AM-N5

THREE DIMENSIONAL STRUCTURE OF BEEF HEART MITOCHONDRIAL CYTOCHROME bc_1 COMPLEX.((D. Xia, C. A. Yu, J. Deisenhofer, J-Z. Xia and L. Yu)), Howard Hughes Medical Institute and University of Texas, Southwestern Medical Center at Dallas, TX 75235 and Oklahoma State University, Stillwater, OK 74078.

The cytochrome bc_1 complex from bovine mitochondria is the largest membrane protein complex crystallized so far. It contains ten protein subunits and five redox centers with a molecular weight of 240,000 Da. It plays a central role in cell respiration. The successful crystallization has been reported from several laboratories. Our crystals, grown in the presence of glycerol, diffract X-rays to better than 3 Å under cryogenic conditions. They have the symmetry of the space group $I4_122$ with unit cell dimensions of a=b=153.5 Å and c=597.7 Å. There are eight bc_1 dimers in a unit cell. Phases have been determined to 3.3 Å resolution by the MIR method with two heavy atom derivatives. The electron density clearly shows the transmembrane region with thirteen transmembrane helices. Four high peaks in the electron density and in maps calculated using anomalous scattering data are interpreted as the redox-centers of the bc_1 complex. Two of these sites are 20 Å apart in the transmembrane region and most likely represent the heme irons of cytochromes b_{562} and b_{565}. Another site near the membrane surface and 26 Å away from the nearest b-heme could be the iron-sulfur center; the fourth site, presumably the cytochrome c_1 heme is 31 Å apart from this center. The majority of the molecular mass outside the membrane is located on the side of the membrane opposite from the redox centers, presumably the matrix side of the mitochondrial membrane. Supported by a grant from the NIH (GM 30721 to CAY).

Tu-AM-N6

THE F_oF_1 ATP SYNTHASE UNCOUPLING MUTATION, γMET-23→LYS, FORMS AN ADDITIONAL CHARGE INTERACTION TO A β SUBUNIT AND DISRUPTS THE STABILITY OF THE $\alpha_3\beta_3\gamma$ COMPLEX.
((M. K. Al-Shawi and R. K. Nakamoto)) Department of Molecular Physiology and Biological Physics, University of Virginia, Charlottesville, VA 22908.

The γ subunit γMet-23→Lys energy coupling mutation does not strongly affect transport or catalytic functions and primarily perturbs the linkage between catalysis and transport. We sought to understand the perturbations caused by the mutation in order to understand the mechanism of coupling. When mutant F_1 was diluted to dissociate δ and ε subunits, ATPase activity was lost. Affinity for δ and ε subunits was unchanged which suggested that the mutation affected the stability of the catalytically active $\alpha_3\beta_3\gamma$ complex. Arrhenius analysis revealed that the mutant enzyme had a transition state with the $\Delta H^{\ddagger}$ parameter more positive, the $\Delta S^{\ddagger}$ less negative and the $\Delta G^{\ddagger}$ unchanged, when compared to wild type. These results suggested that an additional bond was formed that had to be broken to achieve the transition state. Isokinetic analysis indicated that the general reaction scheme had not changed and that the rate limiting step of the mutant enzyme cycle was the same as wild type. The recently solved structure of the F_1 ATPase suggested that a lysine in place of γMet-23 was likely to form an extra charge interaction with βGlu-381 on one of the three β subunits. Moreover, the second-site mutation γArg-242→Cys which eliminated another charge interaction with the same β subunit residue, resulted in stabilization of the enzyme complex and the restoration of efficient coupling. These results suggested that formation of the additional β–γ interaction was the principle cause for the observed changes in F_oF_1 properties, including uncoupling. Supported by PHS grant GM50957.

Tu-AM-N7

FORMATE IS NOT BOUND AS A BRIDGE IN THE SLOW FORM OF CYTOCHROME C OXIDASE FROM BOVINE HEART.
((S. Yergul and G.M. Baker)) Northern Illinois University, Department of Chemistry, DeKalb, IL 60115. (Spon. by AHA, IL Aff.)

The binding of formate to rapid enzyme induces an apparent blue shift in the Soret band and a conversion to the slow form. The blue shift (measured as an absorbance increase at 414 nm) is biphasic at $[HCOO^-]$ / [heme A] ≥ 2×10^3, and can modeled by a two stage reaction of the form $E_0 \rightleftharpoons E_1 \rightleftharpoons E_2$. The fast phase is first order in formate and the slow phase is zero order, indicating that only 1 formate is bound in the overall conversion of E_0 to E_2. The observed equilibrium dissociation constant, $K_{D,f}^{app}$ is 0.1 ± 0.03 mM. From this, we can calculate $k_{d,f}$, the dissociation rate constant for the slow step, as $1.1 \times 10^{-5} \pm 4.2 \times 10^{-6}$ s^{-1}. The binding site of formate has been probed with cyanide. It is now accepted, based on FTIR analysis, that CN^- forms a bridge between Fe_{a3} and Cu_B. If formate is present as a bridge, then subsequent binding rates with CN^- should be limited by $k_{d,f}$ when $k_{a,c}[CN^-] = k_{d,f}$. A kinetic analysis shows that k_{obs} should saturate at ≈ 3 mM CN^-, yet it depends linearly on $[CN^-]$ over the 1 - 150 mM range. We conclude that formate is not bound as a bridge in the slow form.

Tu-AM-N8

BIOCHEMICAL AND BIOPHYSICAL CHARACTERIZATION OF NADH:UBIQUINONE OXIDOREDUCTASE FROM PURPLE BACTERIA; IN SEARCH OF A MODEL SYSTEM TO STUDY ENERGY COUPLING. ((C.Hägerhäll, V.D.Sled, F.Daldal and T.Ohnishi)) Univ. of Penn., Philadelphia, PA 19104, USA,

Purple bacteria have been extensively studied with regards to their primary photochemistry and bioenergetics but rather little is known about coupling site I (NDH-1, Complex I). When grown aerobically their respiratory chain is very similar to that of the mitochondria. EPR features of the iron-sulfur clusters seems to be very similar to their mammalian equivalents. The chromatophores can be made tightly coupled, and in addition the carotenoid band shift can be used as an internal probe to monitor the energetic state of the membrane under various conditions. Furthermore, genetic manipulations can be utilized. Thus purple bacteria provide an excellent experimental system to address how electron transfer is coupled to proton translocation in NDH-1 and to improve understanding of the membrane part of the enzyme. We have compared NDH-1 in chromatophores from *Rhodobacter sphaeroides, Rhodobacter capsulatus* and *Rhodospirillum rubrum* with respect to enzymatic properties, inhibitor sensitivity and enzyme stability. EPR characteristics and redox properties of the iron-sulfur clusters were investigated *in situ* and in partially purified preparations. Methods and preliminary data are presented. (Supported by NIH grants GM 30376 to T.O. and GM38237 to F.D.).

BIOPHYSICAL APPROACHES TO PRESYNAPTIC TERMINALS

Tu-PM-Sym-1

MICRODOMAINS OF ELEVATED Ca^{2+} CONCENTRATION DUE TO CLUSTERED ION CHANNELS AT PRESYNAPTIC ACTIVE ZONES OF HAIR CELLS FROM THE BULLFROG'S INTERNAL EAR. ((A. J. Hudspeth and N. P. Issa)) Howard Hughes Medical Institute and Laboratory of Sensory Neuroscience, The Rockefeller University, New York, NY 10021-6399.

Ca^{2+} channels mediate two critical processes in hair cells, the mechanoreceptors of the auditory and vestibular systems. First, synaptic signaling from such a cell to afferent nerve fibers depends upon the influx of Ca^{2+} at presynaptic active zones. Second, a hair cell's responsiveness is tuned to a specific frequency of stimulation by electrical resonance, which involves an interplay between currents borne by Ca^{2+} channels and Ca^{2+}-activated K^+ channels.

By simultaneously monitoring the whole-cell Ca^{2+} current and the rise and fall of fluo-3 fluorescence intensity, we measured the time course of Ca^{2+} entry, accumulation, and diffusion in hair cells isolated from the bullfrog's sacculus. Upon membrane depolarization, the Ca^{2+} concentration approximately 200 nm from the presynaptic membrane approached a steady state with a time constant of less than 10 ms. Because the sectioning depth of the confocal imaging system exceeded the space constant of fluo-3 fluorescence in the steady state, we developed a numerical procedure to compensate for the effects of out-of-focus fluorescence. Application of this algorithm to fluorescence profiles obtained by rapidly scanning across maximally stimulated active zones indicated that the presynaptic Ca^{2+} concentration reached at least 100 mM. Inclusion in the recording pipette of a Ca^{2+} buffer, such as BAPTA or EGTA, slowed the approach to steady-state fluorescence and restricted the spread of fluorescence from the presynaptic membrane. Both the concentration and the binding rate of the exogenous Ca^{2+} buffer affected the steady-state fluorescence and Ca^{2+} concentration. The observed dynamics of the presynaptic Ca^{2+} concentration is consistent with models of Ca^{2+} entry at and diffusion from a point source.

This research was supported by National Institutes of Health grant DC00241.

Tu-PM-Sym-2

CAPACITANCE MEASUREMENTS OF EXOCYTOSIS AND ENDOCYTOSIS AT A RIBBON SYNAPSE. ((G. Matthews)) Department of Neurobiology & Behavior, SUNY, Stony Brook, NY 11794-5230.

Bipolar neurons are interneurons in the retina that release glutamate from ribbon-type synapses. Ribbons are sheet-like structures found at synaptic active zones in photoreceptors and bipolar neurons and are thought to be a mechanism to increase the population of docked vesicles at the output site. The retina of the goldfish contains a class of bipolar neuron with giant synaptic terminals (10-12 μm in diameter) that are well-suited for patch-clamp analysis of presynaptic mechanisms. In single isolated giant terminals, regulation of membrane fusion and membrane retrieval has been investigated by monitoring the associated changes in membrane capacitance. Activation of presynaptic calcium current induces a rapid increase in capacitance, which reaches a maximum amplitude of about 150 fF within 200 msec. This capacitance response has properties consistent with the rapid exocytosis of a limited pool of synaptic vesicles. Electron microscopy shows that the average vesicle diameter is about 29 nm, so this readily releasable pool corresponds to about 6000 synaptic vesicles. This likely represents the total population of vesicles tethered to the ~55 synaptic ribbons in the terminal. The initial rate of fusion of this pool exceeds 40,000 vesicles per sec. After a bout of exocytosis has been stimulated by a brief depolarization, the added membrane is retrieved with an exponential time constant of 1-2 sec under normal conditions. When resting [Ca] is elevated, retrieval slows dramatically (half-inhibition at 500 nM) and stops altogether when internal calcium exceeds about 1000 nM.

Tu-PM-Sym-3

KINETICS OF THE SYNAPTIC VESICLE CYCLE. ((T. Ryan)) Stanford University.

Tu-PM-Sym-4

TRANSMITTER RELEASE AND SYNAPTIC PLASTICITY IN THE MAMMALIAN BRAIN. ((S.A. Siegelbaum and V.Y. Bolshakov)) HHMI, Ctr. for Neurobiology and Behavior. Columbia University, New York, NY 10032.

Excitatory synaptic transmission in slices of rat hippocampus were studied between an individual presynaptic CA3 pyramidal neuron and an individual postsynaptic CA1 pyramidal neuron. Quantal analysis of the unitary excitatory postsynaptic current (EPSC) recorded from the CA1 neuron (whole- cell voltage-clamped at -70 mV) in response to firing an action potential in a single CA3 neuron (using whole-cell or loose-patch stimulation) shows only two peaks in the EPSC amplitude histogram: one at 0 pA, corresponding to failures of transmission, and one at around -4 pA, corresponding to successes of transmission. Thus, transmission at this synapse appears to be mediated by the release of only a single quantum of transmitter, producing a quantal response of around -4 pA. From the area under the success peak, we estimate that the probability of release, p, in neonatal rats (p4-p8) is around 0.9. Surprisingly, in older rats (p14-p21) p is lower and ranges from 0.1 to 0.5. Quantal analysis was used to investigate the mechanism of long-term potentiation (LTP), an activity dependent increase in synaptic transmission. For its first 30 minutes, LTP is due to an increase in p with no change in quantal amplitude or in the number of release sites. A late phase of LTP, which depends on protein synthesis, is associated with both an increase in p and the appearance of new release sites, suggesting a possible structural change.

K CHANNELS - REGULATION/EXPRESSION

Tu-PM-A1

ALLOSTERIC REGULATION OF K^+ SECRETION CHANNELS BY EXTRACELLULAR K^+ AND INTRACELLULAR PH

((B. Fakler, T. Doi, U. Schulte, H.-P. Zenner, F. Lang and J. P. Ruppersberg)) Dept. of Sensory Biophysics, ENT-Hospital of the University of Tübingen, Röntgenweg 11, 72076 Tübingen, Germany

The K^+ channels which control K^+-homeostasis by mediating K^+ secretion across the apical membrane of renal tubular cells have recently been cloned and named ROMK1, 2 and 3. For the native apical K^+ channels indirect regulation by the K^+ concentration at the basal membrane has been described which involves a cascade of intracellular second-messenger processes. Using heterologous expression in *Xenopus* oocytes together with two-microelectrode recording and giant-patch-clamp technique we show, that ROMK1 (K_{ir} 1.1) channels are directly regulated by extracellular (luminal or apical) K^+ concentration and that K^+ regulation is coupled to intracellular pH. Both, K^+-regulation and its coupling to pH, were assigned to different structural parts of the channel protein: (i) K^+ regulation is removed by introducing a negatively charged residue in the second hydrophobic segment (N171D) previously shown to be involved in inward rectification; (ii) decoupling from pH was achieved by exchanging the N-terminus of ROMK1 by that of the pH-insensitive channel IRK1 (K_{ir} 2.1). These results suggest an allosteric regulation of ROMK1 channels by extracellular K^+ and intracellular pH, which may represent a novel link between K^+-homeostasis and pH control.

Tu-PM-A2

MUSCARINIC MODULATION OF INWARD RECTIFIER CURRENT ((Hong-Sheng Wang, Jane E. Dixon and David McKinnon)) Dept. of Neurobiology, SUNY, Stony Brook, NY 11794

Intracellular recordings were made from rat sympathetic neurons in isolated superior cervical, celiac and superior mesenteric ganglia and neurons were classified as either 'phasic' or 'tonic' (Wang and McKinnon, 1995, J. Physiol., 485:319). An inward rectifier conductance was found to be 6.4 times larger in tonic neurons than in phasic neurons. This conductance was blocked by low concentrations of external Ba^{2+} and Cs^+ ions and had the biophysical properties of a 'strong' inward rectifier.

The inward rectifier was inhibited by synaptic input. Repetitive stimulation of the preganglionic nerve trunk suppressed the conductance by 50-70%. The inhibition had a slow onset of 20-30 seconds, suggesting a second messenger mediated pathway. This synaptically mediated suppression could be mimicked by bath application of muscarine: average peak inhibition 78 ± 1.4%, K_D = 1.95 ± 0.2 μM. Schild plot analysis using the competitive antagonists pirenzepine and himbacine indicated that the effect of muscarine was mediated by M1 muscarinic receptors. By inhibiting the inward rectifier, which contributes a resting K conductance in tonic neurons, synaptic input increases the excitability of these cells.

We have examined the expression of inward rectifier K channel genes in the sympathetic ganglia to determine the gene(s) involved. Components of this neuromodulatory system have been reconstructed in *Xenopus* oocytes to determine the molecular mechanisms underlying this neuromodulation.

Tu-PM-A3

RECEPTOR-DEPENDENT AND -INDEPENDENT COUPLING OF PROTEIN KINASE C TO POTASSIUM CHANNEL INHIBITION.

((L.M. Boland)) Department of Physiology and Neuroscience Program, University of Minnesota Medical School, Minneapolis, MN 55455.

The regulation of potassium (K) channels by protein kinase C was studied in frog oocytes injected with mRNA for voltage-gated K channels of the Shaker subfamily. mKv1.1, rKv1.1 and Shaker H4 (fly) K channels responded similarly in the following experiments. Bath application of phorbol 12-myristate 13-acetate (PMA, 500 nM), an activator of protein kinase C (PKC), caused persistent and complete inhibition of K channel currents. K current inhibition by PMA was blocked by prior injection of channel-expressing oocytes with staurosporine or by bath application of bisindolylmaleimide I, both potent inhibitors of PKC. No inhibition of K channel current was observed in control experiments with PMA analogs that do not activate PKC, including 500 nM phorbol 12-monomyristate and 500 nM 4α–phorbol. To determine whether receptor-dependent PKC activation inhibits K channels, oocytes were co-injected with mRNA's for K channels and P_{2Y} purinergic receptors which have been shown to stimulate phospholipase C. In co-injected oocytes, bath application of the P_{2Y} agonist ATP (100 μM) mimicked the effect of PMA application. These data are consistent with the hypothesis that PKC activation inhibits K channel activity. The molecular basis for this regulation is being explored. (Supported by the Minnesota Medical Foundation.)

Tu-PM-A4

ACUTE MODULATION OF RCK1 DELETION MUTANT CHANNEL BY PROTEIN KINASE A ACTIVATION. ((G. Levin, T. Peretz, D. Chikvashvilli, O. Pongs and I. Lotan)) Dept. Physiol. Pharmacol. Sackler School of Medicine, Tel-Aviv University, Ramat-Aviv 69978, Israel and Zentrum fur Molekulare Neurobiologie, Institut fur Neurale Signalverarbeitung, Hamburg D-20235, Germany.

We have previously shown that the RCK1 (Kv1.1) K^+ channel is a substrate for PKA phosphorylation and identified serin 446 as the target of phosphorylation (Ivanina et al, Biochemistry 33:8786-92, 1994). However, this phosphorylation has only long term effect (Levin et al, J. Biol. Chem. 270:14611-18, 1995), and no acute effect on the channel's function. Here we show that deletion of the N terminus of the channel results in a mutant (RCK1ΔN) that responds to PKA activation by an acute increase in the current amplitude. Preliminary mutagenesis study shows, that this effect is not through serin 446 phosphorylation. Using biochemical analysis, we are currently checking if a direct phosphorylation of RCK1ΔN channel protein is involved in this modulation. We are also checking whether co-expressing the RCK1 wild-type channel with the newly cloned auxiliary β1 subunit (Scott et al, Proc. Natl. Acad. Sci. USA, 91:1637-41 1994) transforms the channel to a PKA-responsive form, as is the deletion mutant.

Tu-PM-A5

KV1.4, KV1.2, AND IRK1 mRNA ARE DIFFERENTIALLY REGULATED IN PRIMARY CULTURES OF FELINE VENTRICULAR MYOCYTES WITH THE RATES OF LOSS OF KV1.4 AND I_{TO} DENSITY BEING COINCIDENT

((Christopher E. Hansen, Robert S. Decker and Robert E. Ten Eick))
Depts. of MPBC & CMB, Northwestern University, Chicago, IL 60611

The density of the myocardial transient outward K current (I_{to}) is affected by cardiac hypertrophy, failure, and ischemia, conditions associated with an increased risk of sudden-death. Both increases and decreases in I_{to} have been reported. Other electrophysiological studies have suggested that the other major components of the cellular membrane current are not significantly changed by these disease conditions. These findings suggest that an understanding of the regulation of I_{to} expression might be important for an improved understanding of the mechanism(s) of sudden death associated with these diseases. We have previously reported that the mRNA encoding for Kv1.4, a candidate gene for I_{to} expression, decreased in feline ventricular myocytes maintained in primary culture with a time course which was almost coincident with the loss of I_{to} density. Since this report, we have now determined that both IRK1 mRNA (for I_{K1} expression) and Kv1.2 mRNA do not significantly decrease in primary culture. Therefore, our results indicate that 1) IRK1 and Kv1.2 mRNA are regulated differentially from Kv1.4 mRNA in primary culture, and 2) only the decrease of Kv1.4 mRNA correlates to the decrease in I_{to} density, suggesting that Kv1.4 may have an important role in the molecular basis of the feline I_{to}.

Tu-PM-A6

MODULATION OF THE ACTIVATION GATING OF hKv1.4 BY A NOVEL β-SUBUNIT FROM HUMAN HEART.

((Z. Wang, A.M. Brown, and B.A. Wible))
MetroHealth Campus, Case Western Reserve University, Cleveland, OH 44109

β-subunits increase the functional diversity of K^+ channels in human heart. Previously, we cloned a β-subunit from human atrium, hKvβ3, which is identical to rat Kvβ1 over the carboxyl-terminal 329 amino acids but has a nonhomologous N-terminal 79 amino acids. These two clones suggest that there might be a family of functionally distinct β-subunit proteins with identical C-terminal regions but different N-termini. We searched for β-subunit sequences expressed in human heart by 5'-RACE using oligonucleotides encoding portions of the conserved C-terminal regions and identified a novel K^+ channel β-subunit, hKvβ4. Full length hKvβ4, obtained from human heart RNA by RT-PCR, is identical to Kvβ1 and hKvβ3 over the C-terminus but possesses a unique N-terminus of 91 residues. Functional expression of hKvβ4 in Xenopus oocytes by coinjection with various K^+ channel α–subunits showed that hKvβ4 modulates hKv1.4 currents, but not hKv1.1, hKv1.2, hKv1.5, or hKv2.1. hKvβ4 affects the activation gating of hKv1.4 as reflected in the delay of current onset and subsequent slowing of the late phase of activation. Both effects were accentuated with hyperpolarizing pulses. In addition, the steady-state activation curve was shifted to more positive potentials by hKvβ4. This modulation is in marked contrast to the action of the other K^+ channel β-subunits which primarily affect the inactivation of selected Kv1 channels. Using the yeast two-hybrid system, we have shown that hKvβ4 specifically associates with the N-terminus of hKv1.4. (Supported by an M.R.C. Fellowship [Z.W.], HL 36930 [A.M.B.], and AHA-Northeast Ohio Affiliate [B.A.W.])

Tu-PM-A7

A NOVEL K^+ CHANNEL REGULATORY SUBUNIT CONFERS RAPID INACTIVATION AND ALTERED VOLTAGE-DEPENDENCE.

((T. Jegla and L. Salkoff)) Department of Anatomy and Neurobiology, Washington University School of Medicine, St. Louis, MO 63110.

We have cloned a novel regulatory α-like subunit (*jShalαR*) for *Shal* K^+ channels from the jellyfish *Polyorchis penicillatus*. Although it is non-functional on its own, *jShalαR* dramatically alters the *jShal1* current when coexpressed in *Xenopus* oocytes. *jShal1* is a highly conserved jellyfish homolog of *Drosophila* and mammalian *Shal* channels, but has relatively slow inactivation and a hyperpolarized activation range. *jShalαR* causes a more than 50-fold increase in the rate of inactivation and an approximately 40mV depolarizing shift in the activation range of this current. The rapid inactivation and the shift of activation range are separable functions conferred by *jShalαR*. The mechanism of inactivation in *jShal1-jShalαR* heteromultimers involves a positively charged N-terminal inactivation "ball", similar to that described for rapidly inactivating *Shaker* and *Shaw* K^+ channels. When this inactivation "ball" region is removed, inactivation is dramatically slowed, but *jShalαR* still shifts the activation range of the *jShal1* current. Although previous studies have shown that heteromultimeric voltage-gated K^+ channels exist *in vivo*, *jShalαR* is the first example of a voltage-gated K^+ channel α-like subunit that appears to be designed to function solely in heteromultimers. Since *jShal1* can function both as a homomultimer and as a heteromultimer with *jShalαR*, it produces two distinct *Shal* currents with radically different properties. *Shal* currents in embryonic neurons from *Drosophila* have similarly varied fast and slow inactivation rates (Tsunoda and Salkoff, *J. Neurosci.*, 1995), and we are presently investigating whether this variation is produced by the same molecular mechanism.

Tu-PM-A8

$G_{\beta\gamma}$ gating of a human pancreatic Kir3.4 channel.

((Diomedes E. Logothetis, M. Noëlle Langan, Jinliang Sui, J. Ashot Kozak, Amanda Pabon and Kim W. Chan)) Department of Physiology and Biophysics, Mount Sinai School of Medicine, CUNY, New York, NY 10029.

GTP-binding (G) proteins have been shown to mediate activation of inwardly rectifying potassium (K^+) channels in cardiac, neuronal and neuroendocrine cells. Functional expression of a recombinant pancreatic inwardly rectifying channel, KGP (a member of the Kir3.4 subfamily), in *Xenopus* oocytes resulted in sizeable basal (or agonist-independent) currents while co-expression with a G-protein-linked receptor, exhibited additional agonist-induced currents. Co-expression of KGP and hbGIRK1 (a human brain homolog of GIRK1/Kir3.1) produced much larger basal currents than those observed with KGP or hbGIRK1 alone. Similarly, when receptor was co-expressed with the KGP and hbGIRK1, large agonist-induced currents were obtained. Pertussis toxin treatment significantly diminished agonist-dependent currents due to KGP or KGP/hbGIRK1 expression. Interestingly, PTX significantly reduced basal KGP or KGP/hbGIRK1 currents as well, suggesting that basal channel activity is also the result of G-protein gating. Specific antibodies recognizing either the KGP or the hbGIRK1 subunit co-precipitated both proteins when co-expressed in oocytes, providing evidence for their heteromeric assembly in the oocyte system. Co-expression of $G_{\beta\gamma}$ subunits with either KGP alone or with the heteromer KGP/hbGIRK1 resulted in significant stimulation of inwardly rectifying currents suggesting that the KGP subunit is gated by $G_{\beta\gamma}$ subunits and thus contributes to the $G_{\beta\gamma}$ gating of the heteromer. We are currently mapping the sites on the KGP subunit responsible for the $G_{\beta\gamma}$ effects.

Tu-PM-A9

ADENOSINE ACTIVATES ATP-SENSITIVE POTASSIUM CHANNELS IN ARTERIAL MYOCYTES *VIA* A_2 RECEPTORS AND CAMP-DEPENDENT PROTEIN KINASE.

((T. Kleppisch and M. T. Nelson)) University of Vermont, Department of Pharmacology, Colchester, VT 05446.

Adenosine is a potent endogenous vasodilator. Activation of ATP-sensitive (K_{ATP}) potassium channels in vascular smooth muscle has been shown to underlie part of adenosine's vasodilatory actions. To examine the mechanism by which adenosine causes K_{ATP} channels to open, whole-cell currents were measured in myocytes enzymatically isolated from rabbit mesenteric arteries. Adenosine induced membrane currents that were inhibited by glibenclamide, a selective blocker of K_{ATP} channels, that were potassium-selective and voltage-independent. Glibenclamide-sensitive currents were also activated by the selective adenosine A_2-receptor agonist, 2-p-(2-carboxethyl)phenethylamino-5'-N-ethylcarboxamido adenosine hydrochloride (CGS-21680). Both adenosine (5 μM, n=37) and CGS-21680 (500 nM, n=12) increased glibenclamide-sensitive potassium currents about 4-fold. The selective adenosine A_1-receptor agonist, 2-Chloro-N^6-cyclopentyladenosine (CCPA) (up to 250 nM, n=12), however, failed to induce potassium currents. Blockers of the cAMP-dependent protein kinase (PKA) effectively inhibited glibenclamide-sensitive currents induced by adenosine and the A_2 receptor agonist. Rp-cAMPS (100-500 μM), an inhibitory analog of cAMP, reduced glibenclamide-sensitive currents in the presence of adenosine by 50.3% (n=5). Similarly, the inhibitor of PKA, H-89 (1 μM), decreased glibenclamide-sensitive currents in the presence of adenosine by 66.7% (n=10). Dialysis of the cell's interior with the highly specific synthetic PKA-inhibitor peptide, PKI(5-24)amide (4 μM), completely abolished activation of potassium currents in the presence of adenosine. These data suggest that adenosine can activate K_{ATP} currents in arterial smooth muscle through the following pathway: (i) Adenosine stimulates A_2-receptors which activates adenylyl cyclase; (ii) the resulting increase in intracellular cyclic AMP stimulates PKA which, probably through a phosphorylation step, opens K_{ATP} channels.

Supported by the Alexander von Humboldt-Stiftung and the NIH

Tu-PM-B1

ANALYSIS OF THE MURINE PHOSPHOLAMBAN GENE PROMOTER IN CULTURED CELLS AND TRANSGENIC MICE. ((V.J. Kadambi, K.L. Koss, K. Haghighi, S. Ponniah and E.G. Kranias)) University of Cincinnati, Cincinnati, OH 45267. (Spon. by James Stout)

Phospholamban (PLB) is an important regulator of myocardial contractility and alterations in PLB expression levels are reflected by alterations in contractile parameters of the heart. To delineate the cis-acting regulatory elements which modulate PLB expression, we initiated PLB-promoter studies *in vitro* and *in vivo*. Two PLB gene constructs containing 7 kb (PLB7CAT) and 2 kb (PLB2CAT) of the region 5'-upstream of the transcriptional start site, were generated. Both PLB constructs contained exon I (88 bp), the intron (6.8 kb), 88 bp of Exon II, and the CAT reporter gene. Transfection of L6 and H9C2 myoblasts (both of which express PLB) with PLB7CAT exhibited ~80% CAT activity relative to pSVCAT (100%). *In vivo* analysis of this construct revealed high levels of cardiac-specific CAT activity in 3 lines of transgenic mice. Furthermore, CAT expression in the ventricle was 3-fold higher than in the atrium in these mice, consistent with the endogenous pattern of differential PLB mRNA expression in these cardiac compartments. Preliminary *in vitro* analysis of PLB2CAT in L6 myoblasts demonstrated ~66% CAT activity relative to pSVCAT. In addition, several lines of transgenic mice carrying the PLB2CAT construct are currently being analyzed. These results demonstrate that PLB7CAT directs cardiac-specific CAT activity, which is differentially expressed between atria and ventricles in transgenic mice. Delineation of the regulatory elements responsible for this differential expression will be important in understanding compartment-specific PLB gene expression in the heart.

Tu-PM-B2

PHOSPHORYLATION AFFECTS THE CONFORMATION, ORIENTATION AND OLIGOMERIZATION OF PHOSPHOLAMBAN. ((Răzvan L. Cornea, Joseph M. Autry†, David D. Thomas, and Larry R. Jones†)) Dept. of Biochemistry, Univ. of Minnesota, Minneapolis, MN 55455, and †Krannert Institute of Cardiology, Indiana Univ., Indianapolis, IN 46202.

β-adrenergic stimulation of phosphorylation of the transmembrane peptide phospholamban (PLB) regulates the sarcoplasmic reticulum Ca-pump in cardiac muscle. Models that have been proposed for the regulatory interaction of PLB with the Ca-pump require modulation of PLB's conformation, net electrostatic charge, and/or pentamerization. We used EPR and FET of recombinant PLB labeled at its cytosolic domain (Lys-3) to detect changes in conformation and orientation of this domain relative to the membrane. EPR of spin-labeled phospholipids was used to measure PLB's oligomeric state as a function of phosphorylation. The membrane topology of spin labels on PLB was estimated based on their accessibility to environment-selective quenchers. We found that phosphorylation leads to a conformational change, possibly a reorientation of PLB's cytosolic domain. The average size of PLB's oligomers in the membrane changes under phosphorylation from 3.5 to 5 for the wild-type species and from 1 to 2 for PLB mutant L37A, a species that is unable to form pentamers in SDS, but regulates the Ca-pump in a manner similar to wild type PLB.

Tu-PM-B3

o-Phthalaldehyde (OPA) modifies the Ca^{2+} release mechanism of skeletal muscle sarcoplasmic reticulum.

((J.J. Abramson[1], S. Koehler[1], S.B. Gopman[1], C.C. Wamser[2], and T.G. Favero[3])) [1]Physics and [2]Chemistry Departments, Portland State University, and [3]Biology Dept., University of Portland.

OPA forms fluorescent isoindoles upon specifically reacting with neighboring cysteine and lysine residues which are spatially separated by ~ 0.3 nm. OPA was shown to induce rapid Ca^{2+} release from SR vesicles, which was inhibited by ruthenium red (μM). High affinity [^{3}H]ryanodine binding was also stimulated by OPA in a biphasic time and concentration dependent manner (< 300 μM). At optimal OPA concentrations, the K_d for ryanodine binding decreased (4 fold), and B_{max} increased (3 fold), while at higher concentrations of OPA, B_{max} decreased rapidly to zero. OPA interacts with two classes of binding sites on the RyR. The high affinity site stimulates binding (in a Ca^{2+} independent manner), while the lower affinity site inhibits receptor occupancy. The fluorescent maleimide CPM does not interfere with OPA's interaction with the RyR. Time dependent fluorescence measurements of OPA binding to the SR show that the formation of the isoindole complex is sensitive to the open vs. closed state of the receptor. SDS-PAGE shows that OPA results in the crosslinking of the RyR, triadin, and FKBP12. OPA is a powerful new covalent probe for studying the interaction between SR proteins during the Ca^{2+} release process. Supported by AHA Oregon Affiliate.

Tu-PM-B4

BINDING LOCATIONS FOR FK506-BINDING PROTEIN ON THE RYANODINE RECEPTOR (RyR) AS DETERMINED BY CRYO-ELECTRON MICROSCOPY. ((T. Wagenknecht, R. Grassucci, J. Berkowitz, H.-B. Xin, and S. Fleischer)) Wadsworth Center, NYS DOH, Albany, NY and Dept. of Molec. Biol., Vanderbilt Univ. Nashville, TN.

A 12-kDa immunophilin (FKBP12) is an integral component of the skeletal muscle RyR. Cryo-electron microscopy and computer image averaging were performed on RyRs prepared by a new procedure in which the endogenous FKBP12 was exchanged with a fusion protein consisting of FKBP12 and glutathione transferase. The averaged image revealed 4 regions of density, attributed to the glutathione transferase, at the periphery of the cytoplasmic component of the RyR. To more precisely map the location of FKBP12, we similarly analyzed and compared micrographs of RyRs containing FKBP12 and of RyRs depleted of FKBP12 (obtained by treatment with the drug, FK590). Four symmetrically distributed regions of density were present in FKBP12-containing RyRs but absent in FKBP12-depleted RyRs. We conclude that FKBP12 binds to the RyR along the edges of the cytoplasmic assembly at a region near the junction of domains "3" and "9" (domain nomenclature defined in Radermacher et al. (1995) J. Cell Biol. 127:411). The FKBP12 sites are about 10 nm from the cytoplasmic end of the transmembrane ion-conducting channel of the RyR. Supported by NIH AR40615 (TW) and NIH HL32711 (SF).

Tu-PM-B5

THREE-DIMENSIONAL RECONSTRUCTION OF A CALMODULIN: RYANODINE RECEPTOR COMPLEX. ((M. Radermacher, Y. Zhou, R. Grassucci, J. Berkowitz, S. Fleischer, and T. Wagenknecht)) Wadsworth Center, New York State Dept. Health, Albany, NY and Dept. of Molec. Biology, Vanderbilt Univ., Nashville, TN (Spon. by W.F. Tivol).

Calmodulin (CaM) modulates the channel activity of the ryanodine receptor (RyR) from skeletal muscle by direct binding. We have determined a three-dimensional reconstruction from electron micrographs of frozen-hydrated CaM:RyR complexes. Under the conditions used to prepare the complexes, the stoichiometry of binding is 4 molecules of CaM per receptor complex. In a previous study (Wagenknecht et al. (1994) Biophys. J. 67:2286) gold clusters were attached to the CaM so that it could be readily detected in micrographs, and the approximate locations of the 4 receptor-bound CaMs was described. Here we have improved the precision of the localization by detecting the CaM directly and by extending the analysis to three dimensions. The 3D reconstruction shows that the center of mass of the CaM is about 3 nm farther away from the transverse tubule-facing surface of the receptor than the location inferred in our previous study. The 4 symmetrically distributed CaM binding sites are about 10 nm from the putative location of the transmembrane ion channel. No major conformational rearrangements occur when CaM binds to the RyR. Supported by NIH AR40615 (TW) and NIH HL32711 (SF).

Tu-PM-B6

NITRIC OXIDE ELICITS CA^{2+} RELEASE FROM SKELETAL SARCOPLASMIC RETICULUM BY OXIDIZING CRITICAL THIOLS ON THE CA^{2+} RELEASE CHANNEL. ((D.A. Stoyanovsky, T.D. Murphy, P. Anno and G. Salama)) University of Pittsburgh, Pittsburgh, PA 15261. (Spon. by E. Levitan)

The oxidation-reduction of critical thiols has been shown to elicit the opening-closure of Ca^{2+} release channels (ie., ryanodine receptors, RyR) of skeletal and cardiac sarcoplasmic reticulum. The addition of $NO^{\bullet}$ donors, nitrosylated cysteine (100-500 μM) or SNAP (S-nitroso-n-acetylpenicillamine) (0.5-1 mM) elicited Ca^{2+} release from SR vesicles in a concentration dependent manner. The release of Ca^{2+} was inhibited by Ruthenium Red (5 μM) and was reversed by addition of a thiol reducing agent (DTT = 1 mM). Superoxide dismutase (SOD) did not modify release induced by NO-donors, indicating that peroxynitrite production was not the primary reactant in this process. SNAP (0.5-1 mM) increased the open-probability of "native" RyRs (SR vesicles fused with planar bilayers), with P_o increasing from 0.2 to 0.9 at pCa 7, but with channel closure at pCa 2.5. Peroxynitrite ($ONOO^-$) and SIN-1 (3-morpholinosydnomine, used to generate $NO^{\bullet}$ + superoxide radical)(at < 1 μM) also elicited SR Ca^{2+} release but could not be reversed by DTT) even though it was partly inhibited by Ruthenium red. These data indicate that $NO^{\bullet}$ and its metabolites act at regulatory thiols on RyRs to modify muscle contraction by mechanisms independent of cGMP pathways.

Tu-PM-B7

THE ACE INHIBITOR, CAPTOPRIL INHIBITS Ca^{2+} RELEASE FROM CARDIAC AND SKELETAL SARCOPLASMIC RETICULUM (SR) BY REDUCING CRITICAL THIOLS ON RYANODINE RECEPTORS (RyR). ((G. Salama, B-R. Choi, M.C. Hein, E. Menshlikova, and J.J. Abramson)), Univ. of Pittsburgh, Pittsburgh, PA 15261 and Portland State University, Portland, OR 97207.

In cardiac and skeletal SR, the oxidation- reduction of critical thiols on the Ca^{2+} release channel elicits the reversible opening and closure of RyRs. In SR vesicles, the oxidation of RyRs by reactive disulfides or free radicals elicited rapid Ca^{2+} release which was reversed by (50-200 μM) captopril. By incubating vesicles with captopril (5-10 min), lower concentrations of captopril (10-50 μM) inhibited Ca^{2+} release induced by sulfhydryl oxidants or semidehydro-ascorbyl radicals. The sulfhydryl oxidants (HOCl (100 μM) and 2,2'dithiodipyridine (10 μM): 2,2'DTDP) are potent inhibitors of [^{3}H]ryanodine binding and their effects were effectively reversed by co-incubation with captopril. However, captopril (0.1-1 mM) alone reduced [^{3}H] ryanodine binding by 17-40%. In Langendorff perfused guinea pig hearts, 2,2'DTDP (20 μM) elicited SR Ca^{2+} release, delayed-afterdepolarizations (DADs), triggered automaticity and ventricular tachycardias (VT) which could be reversed by perfusion with DTT (1-2 mM). Captopril (10-100 μM) in the perfusate did not alter the cardiac action potential or contractility but protected the heart from VT induced by 2,2'DTDP. These data indicate that captopril may be acting as a sulfhydryl reducing agent to protect the heart from thiol oxidation and the ensuing VT.

FOLDING AND SELF-ASSEMBLY: MEMBRANES

Tu-PM-C1

VDAC:A CHANNEL-FORMING PROTEIN WITH AN AUTO-DIRECTED INSERTION MECHANISM. ((X. Xu and M. Colombini)) Dept. Zoology, Univ. of Maryland, College Park, MD 20742.

Triton-solubilized VDAC spontaneously inserts into a planar phospholipid membranes. Zizi *et al.* (J. Membr. Biol. 144:121, 1995) using asymmetric channels, concluded that VDAC channels possess the property of "auto-directed insertion" i.e. they increase the rate of insertion of fellow channels ($> 10^9$) and determine the orientation of insertion. We present direct evidence for catalyzed insertion. We can increase the rate of VDAC insertion into phos-pholipid membranes by 10 to 60 fold by perfusing in 2M urea or guanidinium chloride (GdmCl) into the VDAC-containing side. More strikingly, when the *opposite* side was perfused, the effect was *more* pronounced *and* long-lasting. The urea and GdmCl may change the structure of the pre-inserted channels allowing them to be more effective catalysts for VDAC insertion, or, by flowing through channels they may act on nearby channels inducing them to insert. Either way, insertion *must* be occurring next to the pre-inserted channels. Control experiments showed that water flow, osmotic force, and ionic strength were *not* involved. Nor were the type of phospholipids or the membrane potential. Urea and GdmCl may mimic chaperones by partially unfolding VDAC and keeping it in an insertion-competent state. "Auto-directed insertion" may ensure correct targeting and orientation of nascent proteins *in vivo*.

Tu-PM-C2

CONFORMATIONAL STABILITY OF OUTER MEMBRANE PROTEINS FROM *NEISSERIA MENINGITIDIS*: COMPARISON OF CLASS 2 AND CLASS 3 PROTEINS. ((Conceição A. Minetti[1], Joseph Y. Tai[1], Shu-Mei Liang[1], and David P. Remeta[2])) [1]North American Vaccine Inc., Beltsville, MD 20705, and [2]NHLBI, NIH, Bethesda, MD 20892.

Porins are integral outer membrane proteins responsible for mediating aqueous diffusion of low molecular weight solutes through unique water-filled channel assemblies. These proteins often oligomerize as stable trimers that are resistant to chemical and thermal denaturation. Intra- and interspecies comparisons indicate that this family of proteins share similar structural and functional properties. The major porins from *Neisseria Meningitidis* serogroup B are the mutually exclusive class 2 and class 3 proteins which define bacterial serotyping. Sharing 60 % sequence similarity, these proteins exhibit highly conserved transmembrane spanning ß-sheet domains, whereas serotype-specific epitopes are situated in the variable surface loop regions. Although cross-linking experiments indicate that both proteins adopt native trimeric conformations, only class 2 trimers are SDS-resistant and retain native-like secondary structure in the presence of SDS under ambient conditions. The differential stability with respect to chemical denaturants as monitored by circular dichroism and fluorescence spectroscopy is particularly evident in the presence of Gdn•HCl. Specifically, guanidine-induced unfolding of class 3 and class 2 proteins occurs at transition midpoints of 3.0 M and 5.0 M Gdn•HCl, respectively. Chromatographic and spectroscopic studies suggest that the unfolding/refolding pathways involve population of equilibrium intermediate states. Characterization of these partially folded intermediates in terms of specific secondary/tertiary structural features, thermodynamic properties, and overall conformational stability facilitates elucidation of unfolding/refolding pathways for the class 2 and class 3 proteins within the porin superfamily.

Tu-PM-C3

INSERTION OF *E. coli* α-HAEMOLYSIN INTO PHOSPHOLIPID AND PHOSPHOLIPID-CHOLESTEROL BILAYERS. ((H. Ostolaza, L. Bakás and F.M. Goñi)) Departamento de Bioquímica, Universidad del País Vasco, Aptdo. 644, 48080 Bilbao, Spain).

The water-soluble protein toxin α-haemolysin from *E. coli* (107 kDa) may bind target cell membranes and impair cell function and viability. The binding of the purified toxin to model membranes (liposomes) has been assessed by a direct centrifugation method and by an indirect fluorescent procedure. Binding is independent of the presence or absence of divalent cations, although though α-haemolysin must bind Ca^{++} prior to insertion into the bilayer for membrane lysis to occur. Binding to lipid membranes is also largely independent of lipid composition; toxin-induced membrane leakage is however very sensitive to lipid composition. Studies in which liposomes containing bound protein are incubated with red blood cells, and haemolysis is then assessed, reveal that α-haemolysin binds reversibly lipid bilayers in the gel state, while insertion into lipids in the fluid phase is irreversible.

Tu-PM-C4

INTERACTIONS OF DIFFERENT CLASSES OF AMPHIPATHIC α HELICAL PEPTIDES WITH LIPIDS. ((V.K. Mishra, M. N. Palgunachari, J. P. Segrest and G. M. Anatharamaiah)) UAB Medical Center, Birmingham, AL 35294.

The lipid-associating amphipathic α helices present in exchangeable apolipoproteins have been grouped into different classes based on the distribution of charged residues on the polar face of the helix and other physical chemical properties. Both class A_2 and class A_1 helices have positively charged residues at the polar-nonpolar interface and negatively charged residues at the center of the polar face. However, clustering of the positive and negative residues is less exact in class A_1 compared with class A_2 helices. The class Y helices have two negative residue clusters on the polar face separating the two arms and the base of the Y motif formed by three positive residue clusters. We have studied lipid interactions of 18 residue long model class A_1(Ac-18A_1-NH_2), A_2(Ac-18A_2-NH_2) and Y(Ac-18Y-NH_2) peptides using right-angle light scattering, circular dichroism, fluorescence spectroscopy and differential scanning calorimetry. The observed rank order of lipid affinity of these peptides is: Ac-18A_2-NH_2 > Ac-18Y-NH_2 > Ac-18A_1-NH_2. Since interfacial lysine residues can snorkel and thereby bury their alkyl side chains in the lipid environment, the highest lipid affinity of Ac-18A_2-NH_2 can be explained by largest effect of snorkeling of the exact clusters of the interfacial lysine residues.

Tu-PM-C5

WILD TYPE GRAMICIDIN FORMS A HETERODIMER. ((W. L. Duax, B. Burkhart, D. Langs and W. Pangborn)), Hauptman-Woodward Medical Research Institute, Buffalo, NY 14203.

Precise refinement of the three-dimensional structures of two crystal forms of wild type gramicidin reveal the presence of heterodimers. The refinements clearly reveals the presence of tyrosine residues at position eleven on only one strand of the antiparallel double helix. The approximate ratio of 11-tyrosine to 11-tryptophan in the heterodimer agrees with typical estimates for the ratio of gramicidin C to gramicidin A in wild type gramicidin. The environments of the 11 substituents in the two crystal forms are distinctly different and include specific interactions with solvent molecules. The presence of a heterodimer in crystal forms having significantly different crystal packing suggests that heterodimer formation is a property of the gramicidin and not induced by crystal formation. In our hands, efforts to crystallize pure gramicidin A have invariably failed and crystals prepared from wild type gramicidin do not readily redissolve upon addition of more solvent. The heterodimer appears to be the most stable form of gramicidin and is critical to crystal nucleation. These properties of a gramicidin heterodimer may relate to analogous properties of killer toxin KP6 and prion. Killer toxin KP6 produces K^+ leakage leading to cell death. Although α and β subunits of KP6 are known to be required for toxicity, a stoichiometric mixture is not required. Trace amounts of either will activate the process. The enigmatic behavior of prions, the protein responsible for diseases such as *scrapie* in animals and kuru and Creutzfeldt-Jakob disease in humans, has been attributed to the presence of trace amounts of mutants that induce heterodimer formation or another type of aggregation. Supported by NIH grant GM32812

Tu-PM-C6

RECONSTITUTION OF THE β-CELL ATP-SENSITIVE K^+ CHANNEL. ((John P. Clement IV[1], Gabriela Gonzalez[1], Colin Nichols[2], Susumu Seino[3], Joseph Bryan[1] and Lydia Aguilar-Bryan[1])) [1]Baylor College of Medicine, Houston, TX, [2]Washington University School of Medicine, St. Louis, MO, and [3]Chiba University School of Medicine, Chiba, Japan.

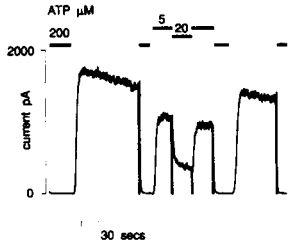

β-cell I_{KATP} has been reconstituted from an inactive small inward rectifier (Kir6.2) = $K_{ATP-\alpha}$, and the sulfonylurea receptor (SUR) = $K_{ATP-\beta}$. Expression of either subunit alone in COSm6 cells generates no K^+ channels measurable by either $^{86}Rb^+$ efflux or single channel methods; co-expression produces a weakly rectifying, K^+ conductance inhibited by ATP (K_i ~ 8 μM) and sulfonylureas (glibenclamide, K_i ~ 2 nM) and activated by diazoxide (K_{act} ~ 65 μM). $K_{ATP-\beta}$ has two nucleotide binding folds (NBFs), mutations in these block I_{KATP} indicating $K_{ATP-\beta}$ is the nucleotide sensor. Deletions of NBF-2 are linked to familial hyperinsulinism (FH), a disorder of newborns characterized by hyperinsulinemia despite severe hypoglycemia. Co-expression of a similarly truncated hamster $K_{ATP-\beta}$, gives 5% of wild type $^{86}Rb^+$ efflux. The data indicate I_{KATP} is a heteromultimeric channel consisting of a minimum of two subunits.

Tu-PM-C7

HIGH-LEVEL EXPRESSION OF CLONED K_{ATP} CHANNELS: MILD INWARD RECTIFICATION DUE TO Mg^{2+} AND POLYAMINE BLOCK. ((S.-L. Shyng, J.P. Clement IV*, L. Aguilar-Bryan*, J. Bryan* and C.G. Nichols)) Department of Cell Biology and Physiology, Washington University School of Medicine, St. Louis, MO 63110, and Department of Cell Biology, Baylor College of Medicine, Houston, TX 77030

Recombinant K_{ATP} channels were expressed in COSm6 cells after transfection with cloned sulfonylurea receptor (SUR) and B-cell inward rectifier (BIK, Kir6.2) channel subunits (Inagaki et al. *Science*, 1995, In Press). Transfection resulted in high-level expression of K_{ATP} channels (> 1000 per patch). Fig. 1 shows current-voltage (I-V) relationships from an inside-out membrane patch

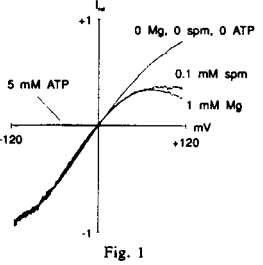

Fig. 1

obtained using voltage ramps from -115 to +115 mV. In the absence of internal polyvalent cations, the I-V is sigmoidal. In the presence of 1 mM Mg^{2+}, or 100 uM spermine^{4+} (spm), a mild inward rectification is induced, that can be explained by assuming a blocking site for each ion, positioned 33% and 16% through the voltage field, respectively. The Mg^{2+} sensitivity matches that of native K_{ATP} channels.

Tu-PM-C8

EFFECTS OF INTEGRAL MEMBRANE PROTEIN ASSOCIATION ON THE RED CELL MEMBRANE ELASTICITY ((Si-shen Feng and Robert C. MacDonald)) Department of Biochemistry, Molecular Biology and Cell Biology, Northwestern University, 2153 North Campus Drive, Evanston, IL 60208.

The remarkable deformability of the red cell membrane has been attributed to the flexibility of spectrin within the membrane skeletal network. Recently, however, evidence has appeared suggesting that alteration in membrane rigidity can be correlated with changes in integral membrane protein organization. As an alternative for the molecular mechanism of the red cell membrane elasticity, a tethered adhesive particle model of two dimensional elasticity is developed. The system considered consists of a planar array of self adhesive particles attached to nearest neighbors with flexible tethers. The particles represent the aggregates of band 3, which are coupled via ankyrin to the spectrin network. The tethers correspond to spectrin tetramers, which restrict the displacement of the particles on the membrane plane and to transmit external stretching forces. For mathematical simplicity, the tethers are considered to have only two states: either fully stretched or completely folded. Analysis of membrane thermodynamics and mechanics results in a constitutive stress-strain relation of the membrane in shear deformation. The shear modulus is deduced to be $\mu_s = \sqrt{N_p q/2l}$, where N_p is the area density of ankyrins, l is the length of the spectrin tetramer and q is the association energy of the band 3 aggregates. The present theory predicts the measured value of $\mu_s = 6 - 9 \times 10^{-3}$ mN/m if $q = 4.0 - 5.9\,kT$.

Tu-PM-C9

INTERPLAY BETWEEN TRANSLATIONAL AND CHAIN CONFORMATIONAL DEGREES OF FREEDOM IN LIPID BILAYERS: A GENERIC PICTURE FOR PHASE BEHAVIOUR ((Morten Nielsen,[1] Ling Miao,[1] John H. Ipsen,[2] Ole G. Mouritsen,[2] and Martin J. Zuckermann,[1])) [1]McGill University, Montreal, PQ, H3A 2T8, Canada; [2]The Technical University of Denmark, Building 206, DK-2800 Lyngby, Denmark

Lipid bilayers possess two types of fundamental degrees of freedom: translational and acyl-chain conformational degrees of freedom of lipid molecules. Research has largely concentrated on understanding the thermodynamic behaviour of the conformational degrees of freedom. In this study, we focus on the interplay between the two types of degrees of freedom and its effects on bilayer phase behaviour by developing a simple microscopic model which describes the fundamental molecular interaction governing both the translational and conformational degrees of freedom; 2) an unconventional 2d off-lattice dynamical triangulation algorithm which allows a realistic, and also computationally efficient, treatment of the translational degrees of freedom. The study of the model by Monte Carlo simulations reveals a generic phase diagram which consists of three principal phases: a solid-conformationally ordered (SO) phase, a liquid-conformationally disordered (LD) phase, and a liquid-conformationally ordered (LO) phase. Depending on the strength of the basic molecular interaction, the system, when thermally driven, can undergo either a first-order transition directly from the SO phase to the LD phase or two consecutive first-order transitions, SO–LO and LO–LD. This prediction offers an explanation to the recent experimental findings of a sub-main transition in a series of phosphatidylcholine bilayer systems (Jørgersen, K., to appear in *BBA*).

Tu-PM-C10

THE STUDY OF BIOMEMBRANE ASSEMBLY DYNAMICS USING COMBINED MESOSCOPIC AND MICROSCOPIC FREE ENERGY MODELS.

((J.G.E.M. Fraaije and B.A.C. van Vlimmeren)) University of Groningen, 9747 AG Groningen, The Netherlands.

We study micro-phase separation phenomena in multi-component biomembrane systems using a dynamic variant of mean-field density functional theory. We propose that the dynamic response of the complex systems can be reduced to a hierarchy of single-chain direct correlator functions. These functions can readily be calculated by Monte Carlo methods. First results indicate that in the non-linear responses cross-correlations can be neglected. The consequences for the dynamics of the biomembrane micro-phase separation processes are under investigation.

Tu-PM-D1

GENERATION OF "ARTIFICIAL" CALCIUM (CA) TRANSIENTS FOR THE STUDY OF CA EXCHANGE WITH CA-BINDING PROTEINS ((J.P. Davis, C.H. Snyder and J.D. Johnson)) Department of Medical Biochemistry, The Ohio State University, Columbus, OH 43210.

Ca transients with ms half widths (h-ws) regulate a variety of physiological phenomena. When slow Ca chelators (EGTA or EDTA ± Mg) are mixed with Ca, "artificial" Ca transients of varying duration and amplitude can be generated in a stopped-flow apparatus. Mixing 200 μM Ca with increasing [EGTA] (0.5-6 mM) yields Ca transients with decreasing duration (h-ws = 11 to ~1 ms at 10°C). Mixing increasing [Ca] (25-400 μM) with 500 μM EGTA created Ca transients with increasing amplitudes and h-ws (from 3 to 15 ms). Mixing 20 μM Ca with 200μM EDTA in the presence of increasing [Mg] (0 to 500 μM) the Ca transients slowed from 4 to 50 ms h-ws, because Mg must first dissociate from EDTA (3 s^{-1}) before Ca can be chelated. An 18 ms h-w Ca transient, like that occuring in a twitch of skeletal muscle, occupies ~100% of the N-terminal Ca specific regulatory sites of S-TnCdanz and dissociates faster than mechanical relaxation. Using TNS fluorescence, a 0.4 ms h-w Ca transient occupied ~ 70% of the N and ~ 20% of the C-terminal sites of Calmodulin (CaM) with Ca. A longer Ca transient of ~ 1 ms occupied ~ 100% of the N and ~ 75% of the C-terminal binding sites of CaM with Ca. Based upon the on and off rates of Ca and Mg for the chelators, proteins and indicators, these artificial Ca transients and fractional occupancies were modeled which agreed with the experimental data. Conclusion: Using these "artificial" Ca transients in a stopped-flow apparatus, it is possible to mimic those Ca transients occuring *in vivo* and determine if Ca exchange with a Ca-binding protein occurs rapidly enough to be physiologically relevant.

Tu-PM-D2

PRIMARY STRUCTURE AND EXPRESSION RATIO OF ALTERNATIVELY SPLICED EMBRYONIC AND ADULT MOUSE SKELETAL MUSCLE TROPONIN T ISOFORMS. ((J. Wang and J.-P. Jin)) Department of Medical Biochemistry, University of Calgary Faculty of Medicine, Calgary, Canada T2N 4N1 (Spon. by G.J. Kargacin).

Troponin T (TnT) is the tropomyosin-binding subunit of the striated muscle troponin complex that participates in the Ca^{2+}-activation of contraction. Multiple isoforms are expressed from the cardiac and skeletal muscle TnT genes through alternative mRNA splicing. To pursue genetic studies on the regulation and functional significance of TnT isoforms, we cloned 30 adult mouse skeletal muscle TnT cDNAs by reverse transcriptase PCR. Sequencing of this large sample of cDNAs revealed the primary structure and expression ratio of seven adult TnT isoforms with a 1:1 ratio of the mutually-exclusive exons 16 and 17, suggesting that they may have a similar functional importance. The alternative splicing frequency of the exons 4 - 8 in the NH_2-terminal hypervariable region of adult skeletal muscle TnT was also determined. Another 30 independent full length TnT cDNA clones were further isolated from a neonatal mouse skeletal muscle library to reveal the primary structure and expression pattern of the embryonic/fetal isoforms. Sequencing results demonstrated an embryonic exon as well as the fetal TnT isoform alternative splicing patterns in both NH_2- and COOH-terminal variable regions. cDNA templates encoding these mouse skeletal muscle TnT isoforms were cloned into a pBV expression vector for genetic expression of the recombinant proteins in *E.coli*. Using the cloned TnT isoforms as control, expression of specific TnT isoforms during development has been demonstrated by Western blotting on both neonatal and adult mouse skeletal muscle protein extracts. (Supported by a grant from the MRC of Canada and a Margaret Gunn Animal Health Research Award)

Tu-PM-D3

ROLE OF TROPONIN T IN THE REGULATION AND COOPERATIVITY OF MUSCLE THIN FILAMENTS. ((M. A. Geeves, S. S. Schaertl & S. S. Lehrer)) Max Planck Institute for Molecular Physiology, Dortmund, Germany & Boston Biomedical Research Institute, Boston, MA.

We previously showed that troponin (Tn) increased the cooperativity whereby myosin subfragment 1 (S1) "turns-on" the actin.Tm thin filament using kinetic studies that monitored both the excimer fluorescence of pyrene-labeled Tm (Tm*) and the light scattering associated with S1 binding. Two effects were produced by binding Tn to actin.Tm*: i) the apparent cooperative unit size, **n**, increased from 6 to 12 actin subunits/S1, and ii) the S1-binding rate constant became Ca2+-sensitive (Geeves and Lehrer, Biophysical J., 67, 273, 1994). We show here that these two effects of Tn can be sepparated by mild proteolytic cleavage of TnT into TnT1 and TnT2, the N- and C-terminal fragments of TnT, respectively. TnT1 and TnT2IC, the complex of TnT2 with TnI and TnC, both bound tightly to actin.Tm*. TnT1 increased **n** from 6 to 9 wihout affecting the apparent rate of binding of S1 to actin.Tm*. In contrast, TnT2IC had no affect on the cooperativity of actin.Tm but did make the S1-binding rate Ca2+-sensitive. Thus, these data indicate that the N- and C-terminal parts of TnT act independently in Tn. The TnT1 part increases communcation between actin.Tm structural units, while the TnT2 part in a complex with TnI and TnC, inhbits the initial binding of S1 to actin in the absence of Ca2+. (Supported by NATO & NIH.)

Tu-PM-D4

COOPERATIVE EFFECTS OF THE TWO HEADS OF HMM IN THE REGULATION OF MUSCLE CONTRACTION. ((S. S. Lehrer & M. A. Geeves)) Boston Biomedical Research Institute, Boston, MA & Max Planck Institute for Molecular Physiology, Dortmund, Germany.

Our previous studies have shown that the excimer fluorescence of pyrene-labeled tropomyosin bound to actin (actin.Tm*) probes the S1-dependent on-off state of the thin filament. When excess ATP is rapidly mixed with S1-saturated actin.Tm* thin filaments, S1 dissociates exponentially (monitored by light scattering, LS). The fluorescence (FI), however, has a lag phase before decreasing exponentially due to remaining heads maintaining the system in the on-state (Geeves & Lehrer, Biophys. J., 67, 273, 1994). In this study a comparison of the stopped-flow kinetics of ATP-induced dissociation of HMM and S1 from actin.Tm* containing 1 bound head/actin subunit, in the presence and absence of ADP, was done to determine if the two heads of HMM act independently. On mixing 10 μM ATP in the absence of ADP, the LS and FI traces were almost identical for HMM and S1 indicating that the heads dissociate independently. On mixing 10 μM ATP in the presence of 1 mM ADP, the HMM system behaved differently from the S1 system. The LS trace showed a long-lived component and the FI trace indicated that the thin filament was maintained in the on-state for a long time. The non-hydrolyzable ATP analogue, ATPγS, was used to determine if cycling heads were required for the ADP-effect in the HMM system. On mixing 290 μM ATPγS in the presence and absence of ADP, normal kinetics were observed in both cases. These data indicate cooperative head effects for HMM in the presence of ADP, whereby one of the two heads maintains actin.Tm in the on-state while the other head undergoes its ATPase cycle. (Supported by NATO & NIH.)

Tu-PM-D5

MOLECULAR MODELING OF ACTOMYOSIN CROSSBRIDGE CYCLE. III. REGULATION OF TROPOMYOSIN-ACTIN-S1 COMPLEX ((P. Dreizen, J. Shi, & C. Shen)) Physiology & Biophysics, SUNY Brooklyn, Brooklyn, NY.

An atomic model for tropomyosin(TM)-actin has been developed in which TM rolls across actin filament from FAR-ON to NEAR-ON to OFF states. The OFF state is characterized by interaction of adjacent lys or arg residues of TM with actin glu334 and asp25, at repeat sites along the actin filament. The TM-actin model is integrated with actin-S1 modeling of weak and strong crossbridges. In weak crossbridges, the interaction of actin 1-4 and S1 loop 627-646 is located ~30Å from OFF-state TM. The S1 head lies adjacent to TM, without steric interference of S1 and TM for actin sites. In activated weak crossbridge, S1 slides across the base of actin 1-28 loop, forming a charge pair lys640-asp25. S1 and TM thus compete for the same asp25 site on actin. Since electrostatic interactions between S1 627-646 loop and actin 1-28 loop are the predominant interactions in weak crossbridges, OFF-state TM may block the transition from weak crossbridge to activated weak crossbridge. In strong crossbridges, S1 moves into the same position occupied by TM in OFF-state and close to TM position in NEAR-ON state. According to this model, addition of S1 drives TM from OFF to NEAR-ON states in absence of Ca^{2+}, and to FAR-ON state in presence of Ca^{2+}. This model is consistent with all relevant evidence including the EM-based steric blocking model; the kinetic data of Chalovich, Greene, Eisenberg, Taylor, and Geeves; and data that formation of regulated A•S1 EDC sites is Ca^{2+}-insensitive in presence of ADP•vanadate or ADP•AlF_x, but Ca^{2+}-sensitive with ADP.

Tu-PM-D6

FUNCTIONAL DUALITY OF THE CENTRAL HELIX IN sTnC: EVIDENCE WITH mini-N AND mini-C TnC FRAGMENTS

((A. Babu Akella, Hong Su, Ernest L. Mehler* and Jag Gulati)) The Laboratory of Molecular Physiology, Albert Einstein College of Medicine, Bronx, NY 10461, & *Mount Sinai School of Medicine, New York, NY 10029

Last year at this meeting, we introduced recombinant N- and C-fragments of rabbit sTnC together with their functional descriptions. The N-fragment (residues 1-102) comprises sites I and II (Ca-specific sites) and the central helix. It could regulate force development in rabbit muscle fiber on activation with pCa4, but could not be anchored in the EGTA solution (no free Ca). Conversely, the C-fragment (residues 73-159), comprising sites III and IV (Ca-Mg sites) and also the central helix, anchored but could not regulate force development. This gave the most direct proof that the N- and C-lobes in sTnC were functionally independent and mutually exclusive. We have now generated mini fragments by deleting the extra central helix. These mini's bound normal Ca (2mol/mol) and were functionally also similar to the long fragments: The *mini-N* (residues 1-83) regulated the force development, and the *mini-C* (residues 91-158) firmly anchored in the absence of Ca. Moreover, the central helix was uninvolved in creating the functional distinctions between the lobes. Further, we compared the washout kinetics of the Ca-saturated N-fragment and *mini-N* from the fiber. The original N-fragment was released rapidly ($t_{\frac{1}{2}}$ = 13±3 min, n=3), but the Ca-saturated *mini-N* lacking the central helix could not be released (up to 2 hr). The results on *mini-N* fragment together with Babu et al. 1993 (JBC, 268,19232-8) indicate a dual role for the central helix structure: In addition to maintaining the minimum separation between the lobes in sTnC, the central helix has an operational function in releasing the trigger domain from the target zone in the fiber. *[Supported by NIAMS/NIH]*

Tu-PM-D7

CONFORMATIONAL CHANGE WITHIN TROPONIN-I IN RECONSTITUTED RABBIT SKELETAL THIN FILAMENTS ((Y. Luo, J.-L. Wu, J. Gergely, & T. Tao)) Muscle Research Group, Boston Biomedical Res. Inst. 20 Staniford St., Boston, MA 02114.

Although much is known about the Ca^{2+}-induced conformational transition in troponin-C (TnC), little is known about how the conformation of troponin-I (TnI) is altered in response to the binding of Ca^{2+} to TnC. In this work we used resonance energy transfer to measure the distance between probes attached at Cys48 and Cys133 in the N- and C-terminal domains, respectively, of TnI under different metal binding conditions. A mutant rabbit skeletal TnI mutant, $TnI^{48/133}$ (C64S), was constructed by converting Cys64 into Ser. The remaining two thiols were labeled with the fluorescent donor 1,5-IAEDANS, and the non-fluorescent acceptor, DAB-Mal. Our results show that the distance between Cys48 and Cys133 was ~40 Å for both uncomplexed TnI, and TnI in the binary complex with TnC. This distance increased to 50 Å in the ternary troponin (Tn) complex with TnT. These distances did not change significantly on binding of Ca^{2+} to the N-terminal triggering sites of TnC. In the reconstituted thin filament, this distance remained 50 Å in the presence of saturating Ca^{2+}, but increased to >65 Å on removing Ca^{2+} with Mg^{2+}/EGTA. Our results indicate firstly that while TnC has only small effects on the conformation of TnI, the additional presence of TnT in the ternary Tn complex results in an apparent elongation of TnI. Secondly, in the inhibited state the stronger interaction between TnI and actin gives rise to a further increase in separation between the TnI domains. (Supported by NIH AR21673 and HL05949)

CARDIAC ION CHANNELS

Tu-PM-E1

BIOPHYSICAL PHENOTYPES OF MUTANT SODIUM CHANNELS IN THE CHROMOSOME 3-LINKED LONG QT SYNDROME. ((Robert Dumaine, [a] Qing Wang, [a]Mark T. Keating, [b]Hali. A. Hartmann, Arthur. M. Brown, Glenn. E. Kirsch.)) Rammelkamp Center for Research, MetroHealth Campus. Case Western Reserve University, Cleveland OH 44109-19989; [a] University of Utah Health Science Center, Salt Lake City Utah 84037; [b]Baylor College of Medicine, Houston TX 77030.

The inheritable long QT syndrome (LQTS) is a disease in which delayed ventricular repolarization is associated with cardiac arrhythmias, characterized by "torsades de pointes" and sudden death. Recently, three changes in the amino acid sequence of the cardiac sodium channel have been identified for chromosome 3-linked LQTS: A three-residue deletion at positions 1505-1507 (ΔKPQ), and two single residue substitutions (N1325S and R1644H). We first tested the hypothesis that mutant channels participate in the prolonged repolarization phase via an increased contribution of inward current in the action potential plateau region. Using heterologous expression in *Xenopus* oocytes, we found that all three mutations failed to inactivate completely, producing a slowly-inactivating, late tetrodotoxin- and mexiletine-sensitive inward current between -20 and 20 mV. We also tested for a contribution to the "torsade de pointes" mechanism by looking at changes in the recovery from inactivation, likely to potentiate premature action potentials and early afterdepolarizations. We found that R1644H and ΔKPQ reprimed three to ten times faster at potentials between -80 and -60 mV while N1325S did not show significant changes. At the single channel level, our results indicate that both destabilization of the absorbing inactivated state and more frequent entry into a "slow" gating mode underlie the late currents. Destabilization predominates over mode shifts in N1325S and R1644H, whereas roughly equal contributions were observed in ΔKPQ. Thus, multiple biophysical mechanisms are responsible for the *in vitro* phenotype of persistent inward current in sodium channel-linked LQTS. Supported by NIH grants NS29473 (G.E.K.), HI37044 (A.M.B.) R. D. was supported by postdoctoral fellowships from the Heart & Stroke Foundation of Canada and Le Fonds de Recherche en Santé du Québec.

Tu-PM-E2

MOLECULAR PHARMACOLOGY OF AN INHERITED HEART DISEASE ((R. Bangalore, R-H. An, R. S. Kass)) Department of Physiology, University of Rochester School of Medicine and Dentistry, Rochester, NY 14642. (Spon. by Kevin Gingrich).

The congenital long QT syndrome (LQTS) is predominantly an autosomal dominant disorder that is characterized by prolongation of the ventricular action potential as well as a propensity to ventricular tachycardia (torsade de pointes) and sudden death. One form of the disease, LQT-3, has been found to be linked to a specific mutation in SCN5A, a gene that encodes the α subunit of the cardiac sodium channel and causes deletion of three amino acids in the III-IV cytoplasmic linker (ΔKPQ) (Wang, et al., *Cell* 80: 805-811, 1995). We have studied pharmacological properties of channels encoded by wild-type (WT) and mutant (ΔKPQ) cDNA's in transiently-transfected HEK 293 cells. Our results show that, in mammalian cells as in *Xenopus* oocytes (Bennett, et al., *Nature* 375: 583-585, 1995), the ΔKPQ mutation encodes Na^+ channels that fail to inactivate completely during prolonged depolarization, underlying a maintained inward current . We find that maintained current through ΔKPQ channels is approximately twice as sensitive to lidocaine block as peak inward current through either WT or ΔKPQ channels. We also find that ΔKPQ mutation speeds both the onset of, and recovery from Na^+ channel inactivation. Lidocaine slows the recovery from inactivation of both WT and ΔKPQ channels such that, in the presence of lidocaine ΔKPQ channels recover with a time course similar to WT channels under drug-free conditions. These results strongly suggest that lidocaine can be used as an effective therapeutic tool to manage arrhythmias that are specific to carriers of the SCN5A gene mutation that is linked to LQT-3.

Tu-PM-E3

EXPRESSION OF A DOMINANT NEGATIVE POTASSIUM CHANNEL FRAGMENT IN THE HEARTS OF TRANSGENIC MICE PROLONGS THE QT INTERVAL. ((B. London, X. Han*, E. Folco*, and G. Koren*)) Harvard Medical School: Children's Hospital and Brigham & Women's Hospital*, Boston, MA

Many K^+ channels are present in the heart and may contribute to cardiac repolarization. N-terminal fragments of Shaker-like K^+ channels (Kv1.x) multimerize with and inhibit related cardiac K^+ channels *in-vitro* in a dominant negative manner (Neuron 12: 615-26, 1994). We have engineered transgenic mice that express a dominant negative channel fragment in the heart to study channel function *in-vivo*.

The transgene, N206, codes for the N-terminal cytoplasmic and S1 transmembrane domains of the rat brain K^+ channel Kv1.1. Expression in GH3 cells leads to a stable protein which is found in the membrane (particulate fraction) of the cells. We injected into the pronucleus of fertilized mouse eggs a construct consisting of 1) the α-myosin heavy chain promoter, 2) N206, and 3) an SV-40 poly-A tail. Genomic Southern blot analysis demonstrated 7 founder mice with variable copy numbers of the transgene. Northern blot analysis of the F1 generation confirmed cardiac expression of truncated channel mRNA in 3 transgenic lines. High resolution EKGs demonstrated QT prolongation to >100 msec in several anesthetized F1 mice from the line with the highest level of RNA expression, a finding not seen in controls at similar heart rates (control QT=78±7 msec, range 75-95; HR=200±31 BPM; n=10).

These studies strongly suggest heteromultimerization of the channel fragment with cardiac K^+ channel subunits *in-vivo*, and confirm a role for the Shaker family of K^+ channels in normal cardiac repolarization in the mouse. We are currently studying the expression of the transgene at the protein level, its effects on the ionic currents of single isolated myocytes, and its interactions with native K^+ channels. We will use these 'long-QT-mice' to begin to define the role of specific channel genes in normal cardiac function, and we will test their efficacy as a model for the long QT syndrome and other human arrhythmias.

Tu-PM-E4

ADENOVIRAL-MEDIATED EXPRESSION OF A POTASSIUM CHANNEL MODIFIES CURRENTS, ACTION POTENTIALS AND CONTRACTION IN NEONATAL RAT AND ADULT CARDIOMYOPATHIC CANINE VENTRICULAR MYOCYTES. ((H. Bradley Nuss, Nipavan Chiamvimonvat, David C. Johns, Stefan Kääb, John H. Lawrence and Eduardo Marban)) The Johns Hopkins University School of Medicine, Baltimore, MD

Viral ion channel gene transfer represents a potentially useful strategy to modify cardiac excitation and contraction. We infected ventricular myocytes in primary culture with AdShK, a recombinant adenovirus containing an inactivation-removed, TEA-sensitive *Shaker* K^+ channel gene driven by the RSV promoter. Within 1-3 days of AdShK infection, neonatal rat cardiocytes expressed robust non-inactivating, TEA-sensitive (5 mM) currents (117.0±22.1 pA/pF, at +40mV, n=8). Cells exposed to similar titers of adenovirus (10-100/cell) expressing the lacZ reporter gene exhibited much smaller (8.0±1.3 pA/pF, n=10), predominantly TEA-insensitive currents. Large TEA-sensitive K^+ currents were also recorded in AdShK-infected failing canine ventricular myocytes but not in controls. Stimulated action potentials (0.2 or 0.1 Hz) were markedly abbreviated in AdShK-infected neonatal rat cells (APD_{50}=17±8 ms, APD_{90}=142±80 ms, n=5) compared to uninfected cells (APD_{50}=170 ±44 ms, APD_{90}=290±43 ms, n=9). The plateau potential was concomitantly depressed (-24±11 mV at 10ms vs 34±3 mV in controls). AdShK similarly modified APs in failing canine cells, which have reduced transient outward K^+ current and prolonged APDs. AdShK-infected canine cells rapidly repolarize to a plateau potential of -24±10 mV (n=8, at 100 ms, vs. 24±3 mV in 7 uninfected cells) and exhibit abbreviated APs (APD_{50}=117±46 ms vs 1795±360 ms). The effects of AdShK on APs in both cell types were largely reversed by TEA. Consistent with its ability to reverse AP depression in AdShK-infected cells, TEA increased video-imaged cell shortening by 41% in neonatal rat cells (n=14) and 122% in canine cells (n=3), but had no effect on shortening in uninfected controls. Thus, viral gene transfer can modify excitability and contractility in isolated heart cells, laying the groundwork for gene therapy for arrhythmias and heart failure.

Tu-PM-E5

EFFECTS OF PROTEIN KINASE C ACTIVATION ON THE HUMAN CARDIAC NA$^+$ CHANNEL. ((KT Murray, N-N Hu, JR Daw, H-S Shin, MT Watson, AB Mashburn, and AL George)) Vanderbilt University, Nashville, TN 37232

Voltage-gated Na^+ channels are critical for normal conduction of electrical impulses in the heart. Conditions which reduce Na^+ current (I_{Na}) can slow conduction and facilitate the development of reentrant, life-threatening arrhythmias. We have recently reported that current derived from the major tetrodotoxin-resistant Na^+ channel isoform in human heart, hH1, is modulated by the phorbol ester phorbol 12-myristate 13-acetate (PMA, 50 nM). Additional experiments were performed to investigate the mechanism of this effect. The two-electrode voltage clamp technique was used to record I_{Na} in *Xenopus* oocytes at room temperature 24-48 hrs following cytoplasmic cRNA injection. At a concentration of 10 nM, PMA caused a marked reduction in hH1 current amplitude averaging 57 $\pm$ 15 % (mean $\pm$ SEM; n=6) at 30 min. Cell membrane capacitance also declined, but to a lesser degree (18 $\pm$ 2 % at 30 min) and usually after a significant fall in I_{Na}. The voltage dependence and time course of Na^+ current inactivation were not affected by PMA ($V_{1/2}$ [mV]: pre = -76 $\pm$ 1, post = -76 $\pm$ 1; τ_{peak} [msec]: pre = 0.72 $\pm$ 0.1, post = 0.86 $\pm$ 0.1). However, there was a small but significant shift in the threshold voltage for channel activation to more positive potentials. 4-α PMA (10nM), the inactive stereoisomer of PMA, had no effect on hH1 current; as well, preincubation with the protein kinase inhibitor chelerythrine (20 μM) prevented the effects of PMA; finally, the hydrolyzable diacylglycerol analog OAG (100 μM) also reduced hH1 current, although the effect was slower and less potent than with PMA (n=2-3 each). These results indicate that activation of protein kinase C modulates hH1 Na^+ current; the effects observed with a reduction in current amplitude could potentially play a role in the genesis of cardiac arrhythmias.

Tu-PM-E6

PROTEIN KINASE C AND ADENOSINE SYNERGISTICALLY POTENTIATE THE OPENING OF ATP-SENSITIVE K$^+$ CHANNELS DURING METABOLIC INHIBITION: IMPLICATIONS FOR ISCHEMIC PRECONDITIONING. ((Yongge Liu, Wei Dong Gao, Brian O'Rourke, Eduardo Marban)) Johns Hopkins University, Baltimore, MD

Ischemic preconditioning is a potent cardioprotective mechanism in which brief periods of ischemia paradoxically protect against subsequent prolonged ischemia. Previous work implicates the activation of adenosine receptors, protein kinase C (PKC) and opening of ATP-sensitive K^+ channels ($I_{K,ATP}$). We investigated the effects of PKC and adenosine on $I_{K,ATP}$ and action potentials in rabbit ventricular myocytes. Currents and action potentials were measured using whole-cell patch clamp with 1 MgATP in the pipette. In control cells exposed to 2 mM cyanide (0 glucose), $I_{K,ATP}$ developed after an average of 15.1±2.4 min (n=8). Ten min pretreatment with PMA alone did not significantly alter this latency (11.9±2.0 min, n=8). Since adenosine receptor activation has been shown to play an important role in the preconditioning response, two groups of myocytes were studied with adenosine (10 μM) included during metabolic inhibition. Without PMA, adenosine alone did not affect the latency to develop $I_{K,ATP}$ (12.3±1.5 min, n=8). However, if cells were pretreated with PMA and then subjected to metabolic inhibition in the presence of adenosine, the latency was shortened to 5.5±1.6 min (n=8; $p<0.02$ vs control, PMA alone, and adenosine alone groups). This effect could not be reproduced by inactive phorbol, but could be blocked by an adenosine receptor antagonist. Consistent with the current measurements, action potential duration shortened much more rapidly during metabolic inhibition in the presence of adenosine if the cells were pretreated with PMA. Our results indicate that PKC and adenosine synergistically potentiate $I_{K,ATP}$ and accelerate the shortening of action potentials induced by metabolic inhibition. The observations provide an explicit basis for current paradigms of ischemic preconditioning.

Tu-PM-E7

DISCRIMINATION BETWEEN K_{ATP} AND INWARD RECTIFIER CHANNELS BY CHARYBDOTOXIN (CTX) BLOCK IN HEART CELLS ((M. Davies, R-H. An, J. Kimbrough and R. S. Kass)) Dept. of Physiology, Univ. of Rochester School of Medicine, Rochester, NY 14642. (Spon. by Ted Begenisich)

The molecular architecture of the K_{ATP} channel in heart and other tissues has not been conclusively determined. Candidate K_{ATP} channel clones have been obtained from the cDNA products of PCR using primers directed at pore regions typical of previously cloned inwardly rectifying K^+ channels. We have used the peptide toxin CTX to begin to explore the architecture of the native K_{ATP} channel pore in cardiac cells using patch clamp recordings of channel activity in single guinea pig ventricular cells. We find that externally-applied CTX blocks current through K_{ATP}, but not inward rectifier (I_{K1}) channels. Using whole cell conditions and pinacidil to induce K_{ATP} activity, we find 50% block in 50 nM and 100% block in 100 nM CTX. Whole cell I_{K1} is unaffected by CTX (up to 150 nM). Outside out patch recordings confirmed CTX block of K_{ATP} but not I_{K1} in the absence of pinacidil. K_{ATP} channels were identified by unitary conductance (60 pS) and glibenclamide sensitivity. 50nM external CTX reduces the open probability of the K_{ATP} channel by 51% (n = 4); but inward rectifier channels in the same patches are not affected by CTX. Our results strongly suggest that the external architecture of the K_{ATP} and I_{K1} channel pores differ and that the cloning strategy for K_{ATP} channels can be altered. Instead of targeting a pore typical of inwardly rectifying K^+ channels, our data suggest that it would be more appropriate to target a pore of a channel previously-shown to be CTX-sensitive such as a *Shaker* or Ca^{2+}-activated K^+ channel.

Tu-PM-E8

ACTIVATION OF A NON-SELECTIVE CATION CURRENT MAY DRIVE NET CELLULAR K$^+$ LOSS DURING METABOLIC INHIBITION. ((J.I. Goldhaber, T.K. Duong and J.N. Weiss)) UCLA Medical School, Los Angeles, CA 90095

The etiology of net cellular K^+ loss during myocardial ischemia and hypoxia is uncertain. Although activation of ATP-sensitive K^+ channels (I_{KATP}) has been implicated, selective activation of I_{KATP} with cromakalim did not induce net cellular K^+ loss in intact rabbit ventricle, despite causing APD shortening and increased unidirectional K^+ efflux similar to hypoxia. To test whether concomitant activation of an inward current drives net K^+ loss, we monitored membrane current and intracellular calcium (Ca_i) in patch clamped adult rabbit ventricular myocytes loaded with Fura-2 via the patch electrode during exposure to either CCCP (5 μM) or rotenone (3 μM). Bath and pipette solutions were designed to eliminate K^+ currents, including the Na^+-K^+ pump current, immediately before voltage ramps from +80 to -100 mV were performed at 1 min intervals. Prior to the onset of cell shortening, both metabolic inhibitors activated a time-independent current with a reversal potential averaging -18.9 ± 5.2 mV and a conductance of ~0.14 pS/μm^2 (CCCP) or ~0.45 pS/μm^2 (Rotenone). The current was not blocked by 5 mM Ni or 30 μM TTX, but was nearly eliminated by replacing monovalent cations with N-methyl-D-glucamine. The current was reversible in 6/11 cells upon washout of the metabolic inhibitor. Changes in Ca_i during metabolic inhibition did not correlate with activation of the current. We conclude that metabolic inhibition activates a non-selective cation current which is a candidate for driving net cellular K^+ loss during ischemia/hypoxia.

FLUORESCENCE - PHOSPHORESCENCE

Tu-PM-F1

DETERMINANTS OF THE FLUORESCENCE PROPERTIES OF (1,8) ANS IN SOLUTION AND IN PROTEINS

((*W. R. Kirk, E. Kurian, W. Wessels & F.G. Prendergast*)) Mayo Foundation, Rochester MN, 55905 (Sponsored by W.R. Kirk).

Fluorescence lifetime and spectroscopic analysis was performed on (1,8)Anilino-naphthalenesulfonate (ANS) bound to the Intestinal Fatty Acid Binding Protein (I-FABP), and apo-myoglobin. These data included quantum yield determinations in H_2O and D_2O, calculation of the radiative rate constant from absorption measurements, and anisotropy decays. We compared these results with data from a set of model solvents (dioxane-water and acetonitrile-water mixtures) which reproduce the spectra of the bound ANS species. Our data suggest that the large enhancement of fluorescence quantum yield and increased fluorescence lifetime, relative to water, which occurs upon binding to proteins is a consequence of dynamical factors, specifically, by the decrease of the rate of the internal rotation about the anilino nitrogen-to-naphthyl C-8 bond. From nmr studies, we showed further that the *ground-state* geometry of the phenyl ring in ANS is similar in the protein and solvent systems, while differing in pure water. This in turn suggests that the emissive state, which we assume to be charge-transfer-like, can be deactivated by charge transfer to the bath, which process may effectively couple to this rotation. The wavelength of the emission maximum is only weakly correlated to the lifetime, and seems to be determined by dielectric properties (and perhaps the Marcus' reorganizational energy) of the solvent.

Supported by GM-34847

Tu-PM-F2

ORIENTATIONAL EXCHANGE THEORY FOR FLUORESCENCE ANISOTROPY

((B. Wieb Van Der Meer, S.-Y. Simon Chen and Charles N. Animalu)) Department of Physics and Astronomy, Western Kentucky University, Bowling Green, KY 42101

A model is proposed in which a membrane probe is represented by a flat disk with its transition moments along the long and short symmetry axes. 6 possible orientations are considered with respect to an XYZ coordinate system with the Z-axis along the membrane normal: the disk has its long and short axes along the Z- and X-, Z- and Y-, X- and Z-, Y- and Z-, X- and Y-, or Y- and X- axes, respectively. The reorientational dynamics in an isotropic membrane suspension, is described by 2 order parameters and 9 rotational rates, of which 4 are independent. This model is an extension of the one proposed by Piston et al. (Biophys. J. 56(89)1083). The anisotropy has 6 independent molecular parameters, and contains 5 exponentials. The anisotropy of a rodlike probe has only 2 exponentials + an r_∞-term and contains 3 independent parameters: 1 order parameter and 2 rotational rates. The same is true for the anisotropy of a disklike probe. The theory fits the perylene data in DMPC of Brand et al. very well (data from "Spectr. and the Dynamics of Mol. Biol. Systems", eds. Bayley and Dale, (85)295). Below the phase transition perylene behaves more like a rod, but above this transition it behaves almost like a disk. Our approach is also applicable to the anisotropy of fluorophores attached to proteins and other macromolecules. This work is supported by NASA (NCCW-60.

Tu-PM-F3

AB INITIO ELECTRONIC STRUCTURE STUDIES ON INDOLE AND IT'S WATER COMPLEXES, INCLUDING CALCULATED SPECTRA. ((David K. Hahn and Patrik Callis*)) Department of Chemistry and Biochemistry, Montana State University, Bozeman, MT 59717.

We have carried out ab initio computations of the ground, ^1L_b, ^1L_a, and ^3L_b states of indole using Gaussian 92. Minimum energy geometries with vibrational modes and frequencies were obtained at the CIS/4-31G level for excited states and up to MP2/6-31G** for the ground state. Detailed vibronic absorption and emission spectra give reasonable agreement with experimental band shapes. The triplet state was found to have a small dipole, thereby accounting for the sharpness of the phosphorescence compared to fluorescence. Geometries of the indole:water complex were obtained at the MP2/6-31G** level and corrected for BSSE. Both π and σ complexes were found to be stable, in agreement with jet-cooled spectra.

Tu-PM-F4

A STUDY OF PROTEIN FOLDING WITH TWO-PHOTON FLUORESCENCE CORRELATION SPECTROSCOPY. ((Sudipta Maiti and Watt W. Webb)) Dept. of Applied Physics, Cornell University, Ithaca, NY 14853.

The technique of fluorescence correlation spectroscopy (FCS) [Magde, Elson and Webb, *Phys. Rev. Lett.* 29, 705 (1972)] has been used to determine the hydrodynamic radii of protein molecules as a function of denaturant concentration. FCS requires minuscule amounts of fluorescent protein (<1 picomole) in dilute (nM) solution and measurements are insensitive to the presence of non-fluorescent impurities. The experimental requirements — a small, open, probe-volume and low background with minimal system fluctuations — are provided by two-photon fluorescence excitation (TPE). Exploiting the advantages of TPE and incorporating efficient data collection and computation of mathematical transforms we have developed an automated FCS apparatus that meets these requirements. The diffusion constants of a few fluorescent and fluorescently labeled proteins (e.g. R-Phycoerythrin and Adipocyte Lipid Binding Protein labeled with acrylodan) have been measured as a function of urea concentration. The characteristic decrease of the diffusion constant (i.e., increase of the hydrodynamic radius) caused by unfolding at higher denaturant concentrations has been observed. Other possibilities for measuring the dynamics of protein folding/unfolding from the FCS data are currently under investigation. We are deeply indebted to E. Kurian and F. G. Prendergast for their kind gift of acrylodan labeled proteins.

Sponsored at Developmental Resource for Biophysical Imaging and Opto-electronics by the NIH (RR04224 and RR07719) and NSF (BIR 9419978)

Tu-PM-F5

PROFLUORESCENT SUBSTRATES FOR PROTEASE ACTIVITY DETECTION: GROUND-STATE XANTHENE DIMERS OR RESONANCE ENERGY TRANSFER? ((B.Z. Packard, A. Komoriya, D. Toptygin, and L. Brand)) Oncolmmunin, Inc., College Park, MD and Johns Hopkins University, Baltimore, MD

Resonance energy transfer (RET) has been widely used in biophysics and biochemistry to measure conformational changes, distances, and small molecules binding to macromolecules. It has also been applied to the detection of protease activities. In the latter, a peptide labeled with both a donor and an acceptor fluorophore such that the emission of the former overlaps with the excitation of the latter usually serves as a substrate; the two fluorophores sandwich an amino acid sequence which contains the target cleavage site of the protease. However, it has not always been clear whether quenching of the donor fluorescence observed in the intact peptide is due solely to RET. We have synthesized a series of substrates for the serine protease elastase and have determined that RET plays a minor mechanistic role when up to 92% of the donor fluorescence is quenched. Absorbance and fluorescence spectroscopic data obtained with peptides labeled with only donors or acceptors were compared with heterolabeled substrates both before and after cleavage; results indicate that in a well-designed substrate ground-state dimer formation can be achieved. The present elastase substrate system offers a unique opportunity to examine various physical parameters of probes such as average distances, spatial orientations, and effects on the conformations of both proteins and peptides as well as quenching efficiency in addition to enabling dissection of the relative contributions of RET, ground-state dimerization, and collisional quenching.

Tu-PM-F6

LOW TEMPERATURE ELECTRONIC SPECTROSCOPY OF ADENINE DERIVATIVES ((Lisa A. Kelly and John C. Sutherland)) Biology Department and National Synchrotron Light Source, Brookhaven National Laboratory, Upton, New York 11973.

The ultraviolet and vacuum ultraviolet absorption spectrum (300 - 110 nm) of adenine, along with the N-7 and N-9 methylated derivatives, has been measured in dilute argon matrices at 12 K. The noble gas matrices provide a transparent, non-hydrogen bonding medium for investigating the spectroscopy of the isolated chromophores. The nature and fate of the electronically excited states were probed by time-resolved and steady-state luminescence spectroscopy. For all of the matrix-isolated adenine derivatives, electronic excitation results exclusively in structured phosphorescence from the lowest electronically excited triplet state. Fluorescence is not observed for any of the adenine derivatives in the argon matrices. The spectra of matrix-isolated adenine and 9-methyladenine show phosphorescence maxima at 400 nm, with the spectrum of 7-methyladenine blue shifted *ca.* 25 nm. These results will be compared and contrasted with those obtained in frozen ethanol glasses at 77 K. In the frozen alcohol solvents, both fluorescence and phosphorescence are observed from the lowest lying electronically excited singlet and triplet states, respectively. The lifetime of the former state was measured to be *ca.* 2.0 ns for all of the adenines investigated. The results suggest that the photophysical properties of the adénine chromophore are medium dependent and likely governed by hydrogen bonding to solvent.

This work was supported by the National Synchrotron Light Source, the U. S. D.O.E. Office of Health and Environmental Research, and the U.S. D.O.E. Distinguished Post-Doctoral Fellowship Program.

Tu-PM-F7

Fluorescent Diffuse Photon Density Waves in Turbid Media: Analytic Solutions and Sensitivity Analysis

X. D. Li[†*], M. A. O'Leary[†*], D. A. Boas[†*], B. Chance[*] and A. G. Yodh[†]
[†]*Department of Physics,* [*]*Department of Biochemistry and Biophysics*
University of Pennsylvania, Philadelphia, PA 19104

The past few years have seen increasing interest in fluorescent contrast agents as a means to enhance the specificity and sensitivity in tumor detection [1-3]. The determination of local fluorophore concentration and lifetime may provide useful information about tissue environment. We present analytic solutions for fluorescent diffuse photon density waves originating from fluorophores distributed in thick turbid media like tissues. Solutions are derived for a homogeneous turbid medium containing a uniform distribution of fluorophores, and for a system which is homogeneous except for the presence of a single spherical inhomogeneity. Forward calculations show that $\leq$ 5-fold fluorophore concentration contrast and lifetime variations (within $\sim$ 80%) are sufficient to detect an object of 0.5 *cm* radius centered between the source and detector with 6 *cm* source-detector separation. The relative sensitivities of absorption and fluorescence of fluorophores are also compared using the analytic solutions. Tomographic imaging of concentration and lifetime will also be presented.

[1] E. M. Sevick-Muraca and C. L. Burch, "Origin of phosphorescence signals reemitted from tissues", Optics Letters, Vol.19, No.23, 1928-1930(1994).
[2] M. S. Patterson and B. W. Pogue, "Mathematical model for time-resolved and frequency-domain fluorescence spectroscopy in biological tissues", Applied Optics, Vol.33, No.10, 1963-1974(1994).
[3] C. L. Hutchinson, J. R. Lakowicz and E. M. Sevick-Muraca, "Fluorescence Lifetime-based Sensing in Tissues: A Computational Study", Biophysical Journal, Vol. 68, 1574-1582(1995).

Tu-PM-F8

TUNING ION AFFINITY AND SELECTIVITY OF THE EF-HAND CA^{2+} BINDING MOTIF: CHANGES AT THE GATEWAY POSITION ((S.K. Drake, K.L. Lee and J.J. Falke)) Univ. of Colorado, Boulder, Co. 80309

The ion binding parameters of the EF-hand Ca^{2+} binding motif are carefully tuned for different Ca^{2+} signaling pathways, yielding a diversity of Ca^{2+} binding affinities, selectivities, and kinetics among the numerous proteins of the EF-hand superfamily. The gateway residue of the semi-conserved EF-loop, located at the interface between the ion binding cavity and solvent, controls association and dissociation kinetics, but its effect on the equilibrium parameters are unclear. To examine these equilibrium effects, eight different gateway sidechains in the model EF-loop of the *E. coli* galactose binding protein were characterized for their effects on ion binding affinity and selectivity. Neutral gateway sidechains (Gln, Asn, Thr, Ser, Ala, Gly) have little or no effect on Ca^{2+} affinity of the site, and retain the native ability to exclude Na^+, K^+ and Mg^{2+}. This is consistent with the kinetic tuning model for the gateway position, where the sidechain controls EF-loop activation kinetics independently of the Ca^{2+} binding equilibrium. The present study also examines the ionic charge and size selectivities of the eight model sites using the spherical cations of Groups Ia, IIa, IIIa, and lanthanides. Acidic gateway sidechains (Glu, Asp) are found to shift charge selectivity as much as 10^3-fold toward trivalent cations. Both acidic and neutral sidechain substitutions yield altered size selectivities for nonphysiological cations larger than the optimal radius. The native gateway sidechain (Gln) provides the greatest size selectivity, exhibiting a single optimal radius. All other gateway sidechains cause a partial loss of size selectivity. Overall, the results demonstrate that, in addition to its kinetic tuning role, the gateway sidechain helps define the equilibrium size and charge of the EF-hand ion binding cavity. The molecular mechanisms of size and charge selectivity are discussed.

Tu-PM-G1

ELECTROSTATIC MODEL FOR PROTON PUMPING IN CYTOCHROME C OXIDASE.(H. ROTTENBERG) MCPHU, Philadelphia, PA 19102

Proton pumping in heme-copper oxidases is proposed to be driven by alternating electrostatic charging of the binuclear center. The binuclear center which is located close to the cytosolic surface is connected to the matrix by a hydrogen-bonded hydroxyl wire. The transient negative charge of the binuclear center, after the injection of each electron, push electrons through the hydrogen-bonded hydroxyl wire, from the binuclear center to the matrix surface where hydroxyls are produced (from water), thus generating $\Delta\Psi$ and ΔpH. Hydrogens (not protons) move through the wire from the matrix face to the binuclear center (consumed protons). The negatively charged center also increases the pK of proton acceptors on the cytosolic surface and drive the vectorial protons from an hydronium funnel on the matrix surface, through a different hydrogen-bonded pathway, across the membrane osmotic barrier. The ferryl state, which is postulated to be positively charged, decreases the pK of the acceptors, thus releasing the vectorial protons. The model is compatible with the recently published structure of COX and much of the data regarding the kinetics, thermodynamics, and molecular biology of the heme-copper oxidase family.

Tu-PM-G2

PROTEINS AS SOLVENTS: ROLE OF REMOTE AMINO ACIDS IN THE CHARGE TRANSFER DYNAMICS OF PLASTOCYANINS. ((A. Webb, E. Fraga, G. R. Loppnow)) Department of Chemistry, University of Alberta, Edmonton, Alberta, Canada T6G 2G2.

Plastocyanin is an 11-kDa copper protein involved in electron transport in the photosynthetic apparatus of plants. The rate of electron transport depends on the distance between donor and acceptor, the free energy of electron transfer, the electronic coupling of donor and acceptor, and the reorganizational energy of the donor, acceptor, and solvent. To identify the structural determinants of the reorganization, we have measured the resonance Raman excitation profiles of parsley, spinach, and poplar plastocyanin at wavelengths throughout the S(cys)→Cu(II) charge transfer absorption band at 597 nm. Self-consistent analysis of the absorption spectra and resonance Raman excitation profiles suggests that charge transfer is accompanied by reorganization along primarily S(cys)-Cu stretches with minor contributions from Cu(II)-N(his) stretches, internal cysteine modes, and protein backbone modes. The reorganizational energy contribution from resonance Raman-active modes is estimated to be ~0.2 eV in all three plastocyanins. Comparison of the resonance Raman spectra of parsley, spinach, and poplar plastocyanin suggests that small changes in the protein composition far from the copper site influence the mode-specific charge transfer dynamics. These results are discussed in terms of the role of the environment in electron transfer.

Tu-PM-G3

FABRICATION OF VECTORIALLY-ORIENTED CYTOCHROME OXIDASE MONOLAYERS. ((A.M. Edwards, J.A. Chupa, R.M. Strongin, A.B. Smith, III, and J.K. Blasie)) Department of Chemistry, University of Pennsylvania, Philadelphia, PA 19104. ((L.J. Peticolas and J.C. Bean)) AT&T Bell Laboratories, Murray Hill, NJ 07974.

Vectorially oriented monolayers of detergent-solubilized Bovine Heart Cytochrome c Oxidase have been formed by self-assembly from solution and Langmuir-Blodgett (LB) deposition. Both quartz and Ge/Si multilayer substrates, the latter fabricated by molecular beam epitaxy (MBE), were alkylated with an amine-terminated alkylsiloxane monolayer prior to introduction to the protein. For the self-assembled protein monolayers, the amine endgroup surface provided for primarily electrostatic interactions with the protein, thereby encouraging a near unidirectional vectorial orientation of the so-adsorbed integral membrane protein. This was demonstrated by the analysis of meridional x-ray diffraction data from the monolayers so-adsorbed onto the Ge/Si multilayer substrates, which yields electron density profiles of the protein along the axis normal to the substrate plane. These profiles are consistent with the three dimensional structure obtained from electron microscopy. Initial Patterson function analysis of meridional x-ray diffraction from the LB-deposited monolayers has shown the profile structure of the so-deposited protein monolayers to be qualitatively similar to that obtained via self-assembly from solution, thereby suggesting that the LB-deposited monolayers are similarly vectorially-oriented. Optical spectroscopy using quartz substrates has also indicated that the LB monolayers tend to be more densely packed than their self-assembled counterparts and optical linear dichroism suggests that the normal to the average heme plane lies more parallel to the substrate than for monolayers formed by self-assembly. Such densely packed, vectorially-oriented monolayers are important for a number of related structural and functional studies of single monolayers of Cytochrome Oxidase.

Tu-PM-G4

THEORETICAL STUDY OF THE STRUCTURE AND DYNAMICS OF BIOLOGICAL PROTON WIRES.
((R. Pomès and B. Roux)) Membrane Transport Research Group and Department of Chemistry, University of Montreal, Montreal, Quebec, Canada H3C 3J7

There is growing evidence for the mediation of proton translocation by hydrogen-bonded chains of water molecules, or *proton wires*, embedded in a number of important biological systems. In our work, we have used path integral quantum-classical and classical molecular dynamics simulations to study the structure and the dynamics of protonated chains of hydrogen-bonded water molecules, successively in vacuo and in the gramicidin channel. The properties of the proton wire were characterized, and the complex interplay governing the molecular mechanism of H^+ translocation in hydrogen-bonded systems was analyzed. The flexibility of water-water hydrogen bonds, combined with zero-point energy effects, was found to be essential in modulating the process leading to proton translocation. In addition, the presence of cooperative motions within the water chain appeared to limit the net translocation of H^+ both in vacuo and in the single-file of the gramicidin channel. In these systems, the rate limitation for translocation over several hydrogen bonds was seen to arise from successive thermal fluctuations involving the heavy nuclei of the entire chain. In turn, in biological systems the dynamics of the water wire is affected by the presence of charges and of hydrogen bonds with the protein. In the ongoing study, molecular dynamics simulations are used to characterize the stability and the dynamics of proton wires in bacteriorhodopsin and in the photosynthetic reaction center of *Rhodobacter sphaeroides*.

Tu-PM-G5

ELECTROSTATIC AND HYDROPHOBIC INTERACTIONS DURING COMPLEX FORMATION AND ELECTRON TRANSFER IN THE FERREDOXIN/FERREDOXIN-NADP$^+$ REDUCTASE SYSTEM FROM ANABAENA. ((J.K. Hurley [*], M. Fillat [#], C. Gómez-Moreno [#] and G. Tollin [*])), [*]Department of Biochemistry, University of Arizona, Tucson, AZ, U.S.A. and [#]Departamento de Bioquímica y Biología, Universidad de Zaragoza, SPAIN.

Transient kinetics and protein/protein binding constants (K_d) have been used to characterize interactions occurring during electron transfer (et) from ferredoxin (Fd) to ferredoxin:NADP$^+$ reductase (FNR). K_d for the complex between oxidized Fd and oxidized native FNR decreases slightly between I = 12 mM and 100mM, whereas the K_d for the complex formed by Fd and recombinant FNR increases by four-fold over this same ionic strength range. For both pairs of proteins, the ionic strength dependence of k_{obs} for the et reaction is biphasic, although the native FNR shows a smaller effect at low ionic strengths than the recombinant. The dependence of k_{obs} on FNR concentration is linear for both protein pairs at I = 12 mM, whereas at I = 100 mM the k_{obs} values show saturation behavior with respect to the FNR concentration. Electrostatic analysis of the kinetic data allows a prediction of the ionic strength dependence of the K_d values if electrostatic forces were dominant in determining complex stability. The predicted dependence is dramatically larger than the observed effects of ionic strength, indicating that hydrophobic interactions contribute significantly to complex stability. The kinetic results are explained by assuming that two protein/protein complexes exist, one which is electrostatically stabilized and is nonproductive with regard to et, and a second which is stabilized by hydrophobic interactions and which is productive.The different behavior of the two FNR's is ascribed to proteolysis at the N-terminus in the native enzyme, which is known to occur during preparation and which removes two positively charged residues.

Tu-PM-G6

THE O_2 REACTION OF CYTOCHROME aa_3-QUINOL OXIDASE FROM *BACILLUS SUBTILIS*. ((B.C. Hill)) Department of Biochemistry, Queen's University, Kingston, ON K7L 3N6.

The quinol oxidase from *B. subtilis* plasma membranes is a member of the cytochrome oxidase family. It has a binuclear cytochrome a_3-Cu_B center and low spin cytochrome *a*, but lacks the Cu_A site. The reduced enzyme forms a ferrocytochrome a_3-CO, which limits the reaction of the enzyme with O_2. I have used the flow-flash method to investigate the reaction of the reduced enzyme with O_2. In the visible region it is possible to observe formation of a spectrum with features of an oxy complex of cytochrome a_3. This species decays in a single exponential process to a species with the spectrum of a ferryl state of cytochrome a_3. The form of this reaction has been investigated as a function of pH. The relationship of this reaction sequence to that found for the bovine enzyme will be discussed.

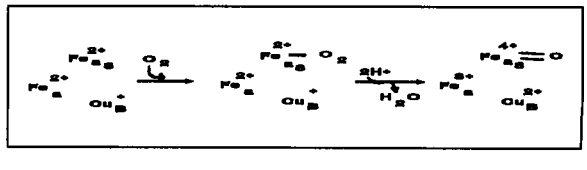

Tu-PM-G7

STRUCTURAL CHANGES INDUCED BY TEMPERATURE IN CYTOCHROME *C* OXIDASE FROM MITOCHONDRIA AND BACTERIA STUDIED BY INFRARED SPECTROSCOPY [(J.L.R. Arrondo, I. Echabe and F.M. Goñi)] Dpto. Bioquímica. Univ.Pais Vasco. P.O.Box 644. 48080 Bilbao. Spain.

Cytochrome *c* oxidase is ubiquitous to all aerobic cells. In prokaryotes is a plasma membrane enzyme whereas in eukaryotes is localized into the mitochondrial inner membrane. In eukaryotes, three subunits are encoded in the mitochondrial DNA and the rest of the subunits in the nucleus. The mitochondrially coded proteins have homologous counterparts in the bacterial enzyme. We have studied the enzymes from mitochondria, *P. denitrificans* and a mutant from this bacteria lacking subunit III. The thermal behaviour of the three proteins is different. Thus, the mitochondrial protein conforms to a two-state denaturation in the range 45-60 °C, with a different behaviour for the band corresponding to α-helix (57 °C) or ß-sheet (48 °C). The *P. denitrificans* enzyme denaturation is accomplished in two steps (43.5 and 54 °C) similarly to the observation made by DSC. Thermal behaviour of the mutant differs from the other proteins. The denaturation temperature of the α-helix and ß-sheet components is alike in the mitochondrial enzyme if the heating is in multiple steps. The presence of detergents or urea also changes the thermal behaviour of the enzyme. The results indicate that inter-subunit interactions play an important role in the denaturation pattern.

Tu-PM-G8

INVESTIGATING THE MECHANISM OF ELECTRON TRANSFER IN SMALL COPPER BINDING PROTEINS: X-ray Crystallographic and Spectroscopic Studies of the Holo and Apoazurin from *Ps. fluorescens*.

((*T. E. S. Dahms, *M. J. Kaminski, ¶J. D. Biesterfeldt, *S. J. Evans, ¶A. G. Szabo & ‡X. Lee)) *University of Ottawa, Ottawa, Ontario, CA K1H 8M5 ¶University of Windsor, Windsor, Ontario, CA N9B 3P4 ‡Cleveland Clinic Foundation, Cleveland, Ohio, USA 44195.

Pseudomonas fluorescens (*Pfl*) azurin is classified as a small "blue copper protein" (λ_{max} = 280 nm, 600-625 nm) which complexes with cytochromes *c*, its redox partner, *in vivo*. Although the "blue copper proteins" have been studied extensively by various biochemical and physical techniques, the complete mechanism of electron transfer is not clear.

X-ray crystallographic data of the *Pfl* holoazurin ($P2_12_12_1$; a = 31.95 Å, b = 43.78 Å, c = 78.81 Å; Z = 1) at 2.05 Å resolution provides a three dimensional structure with the following unique features; a main chain "flip" at His35 and direct involvement of the His35 patch in the contact between symmetrically related molecules. These observations support a structural basis for the electron transfer through the His46-His35 channel to the next molecule which can be used as an approximate model for electron transfer between azurin and cytochrome *c*. Small apoazurin crystals were found to diffract to 2.5 Å resolution, providing sufficient data for the investigation of copper-induced conformational changes.

The structures of the *Pfl* holo and apoazurins will be discussed in detail, highlighting copper ligand geometry and electron transfer. An attempt will be made to grow crystals of the nickel and cobalt derivatives of azurin and the azurin-cytochrome complex. Structural information from these systems would facilitate a comparison of X-ray crystallographic data with that obtained by fluorescence (Hutnik & Szabo (1989) *Biochemistry*, **28**, 3935.), and further define the contact area between *Pfl* holoazurin and cytochrome C. Taken together, this data would more clearly define the electron transfer process *in vivo*.

CONTRACTILITY, LOCOMOTION, MOTILITY: MYOSIN

Tu-Pos1

DETECTION OF REPETITIVE TITIN EPITOPES DEPENDS ON THE LABELLING TECHNIQUE. ((K. Trombitás*, M.L. Greaser^ and G.H. Pollack+)) *Central EM Lab., Univ Med. School of Pecs, Hungary; ^Muscle Biology Lab. Univ. Wisconsin, Medison WI 53706; +Center for Bioengineering, Univ. of Washington, Seattle WA 98195.

A number of monoclonal antibodies against titin have been prepared in several laboratories which label the sarcomere at various positions from M-line to Z-line. Some of the antibodies recognize only a single epitope, but several label repetitive epitopes. Only one known monoclonal antibody (T30) binds to five epitopes with 42 nm spacing in the C-protein zone. Here, we describe work with monoclonal antibody H4 (Fassel and Greaser, 1995) which labels numerous epitopes depending on the labelling technique. This antibody showed two bands per sarcomere with the immunofluorescence method. Using indirect immuno-electron microscopy (anti-mouse IgG as secondary antibody), we found four repetitive epitopes 42 nm apart in each half sarcomere. When the secondary antibody was anti mouse IgG Fab' fragments conjugated with 1.4 nm gold particles, followed by silver enhancement (Nanoprobe Inc.), we could identify seven epitopes. The same four epitopes were accompanied by a fifth epitope 42 nm from the epitope nearest the M-line. Then, about 84 nm closer to the M-line, there appeared two additional epitopes spaced 42 nm apart. The first five epitopes correspond to the epitopes of the T30 antibody, the two additional to the epitopes of the T31 antibody (Fürst et al., 1989), which means that the H4 antibody covers seven epitopes of the nine striations associated with C protein and the 86K protein. Since the labelling showed a steeply decreasing gradient from the periphery towards the core of the fiber, the properly chosen antibody concentration is important for full identification of epitope positions—as is the new supersensitive labelling technique.

Tu-Pos2

A DIRECT DETERMINATION OF THE STEP-SIZE DISTANCE FOR ATP SPLITTING IN ACTIVELY CONTRACTING MUSCLE.

((C.R.Worthington and G.F.Elliott)) Carnegie Mellon Univ., Pittsburgh, PA 15213 and Oxford Research Unit, Open Univ., Oxford OX1 5HR UK.

The rate of energy consumption in muscle contraction and the velocity of shortening as a function of load have long been known from the pioneering work of A.V.Hill. Since those days information has accumulated about the structure of striated muscle and about the enthalpy supplied by each ATP molecule in the contractile process. In principle all this information can be combined to give the distance travelled in contracting muscle by one actin filament past one myosin filament as a result of the hydrolysis of one ATP molecule. This definition of the step-size distance in muscle is independent of any particular model of the physical-chemical process of muscle contraction since it depends only on experimentally determined quantities. We have carried out this calculation and report that the step-size distance on our definition is 1.7 nm at maximum shortening velocity. It decreases with load becoming zero when the force is isometric. The analysis supposes that muscle contracts as a result of a series of impulsive forces and it gives a physical meaning to Hill's constants a & b in Hill's force-velocity equation. Hill's constant b is related to the impulse-time and an estimate of 0.5 msec is obtained. Hill's constant a is related to the inertia of the system and to the viscous-like frictional resistance experienced by the filaments as the muscle shortens. We note however that a recent model for muscle (Elliott & Worthington Bioch. Biophys. Acta 1200, 109 [1994]) fits admirably within the frame-work of the present treatment. Some properties of this electrical model will be described.

Tu-Pos3

ISOLATION OF THE CIRCULAR DICHROISM (CD) SIGNAL FROM TRP510 IN MYOSIN SUBFRAGMENT 1 BY USE OF FLUORESCENCE DETECTED CD (FDCD) ((Sungjo Park, Katalin Ajtai, and Thomas P. Burghardt)) Department of Biochemistry and Molecular Biology, Mayo Foundation, Rochester, MN 55905.

FDCD was used to detect the CD signal from the five tryptophan residues in α-chymotryptic S1. FDCD was detected from native S1, and S1 after specific modification of the fast reacting thiol (SH1) with the fluorescent probe 5'iodoacetamidofluorescein (5'IAF). 5'IAF modifying S1 (5'F-S1) closely interacts with Trp510 of S1 totally quenching the emission from this tryptophan. Other tryptophans in S1 are not affected by 5'IAF[1]. The difference FDCD spectrum between the S1 and 5'F-S1 originates solely from the native structure of Trp510. Calculation of the tryptophan CD signal combined with the α-carbon structure of S1[2] indicates possible native conformation of the residue.
Supported by NIH (AR 39288), American Heart Association (GIA 930 06610), and Mayo Foundation.

1. Ajtai & Burghardt, 1995, Biochemistry, in press.
2. Rayment et al., 1993, Science 261, 50-58.

Tu-Pos4

DISTANCE BETWEEN THE ALKALI LIGHT CHAINS OF MYOSIN SUBFRAGMENT-1 BOUND TO F-ACTIN MEASURED USING FLUORESCENCE SPECTROSCOPY. ((L. Brown & B. Hambly)) Pathology Dept., Sydney University, NSW 2006 Australia.

Fluorescence resonance energy transfer (FRET) spectroscopy was used to measure the distance between a fluorescent donor probe bound to the alkali light chain (ALC) of myosin subfragment-1 (S-1) and an acceptor probe bound to the ALC of an adjacent S-1, when a mixture of these two labeled S-1 molecules was bound to filamentous actin (F-actin) in rigor buffer. No fluorescence quench occurred between this fluorescence probe pair. We calculated the apparent distance between these two fluorophores to be greater than 8.0 nm). Both the donor (N[[(iodoacetyl) amino]ethyl]-5-naphthylamine-1-sulphonic acid [IAEDANS]) and acceptor (5-iodoacetamide fluorescein [5-IAF]) fluorecent probes were bound stoichiometric-ally to the Cys 177 of separate samples of ALC-1 of rabbit skeletal muscle myosin and exchanged onto the α-chymotryptic S-1 fragment of myosin. The extent of labeling of the donor S-1 was 0.93 and the acceptor S-1 was 1.00. Two ratios of donor to acceptor S-1 samples were prepared: (i) 0.2 donor S-1:0.6 acceptor S-1:1 F-actin; (ii) 0.5 donor S-1:0.5 acceptor S-1:1 F-actin. No quenching of fluorescence was seen in either case. Sedimentation binding studies of the fluorescence samples showed that greater than 95% of S-1 had bound the F-actin. The distance between S-1 molecules bound to F-actin that can be predicted from the helical repeat of the F-actin filament is 6 nm. These results will be discussed in relation to the apparent flexibility between the motor domain and the light chain domain of the myosin head, when bound to F-actin in the rigor complex. Supported by the NH&MRC of Australia.